

PREPRINT

Loop-induced masses for the first two generations with optimum flavour violation

Gurucharan Mohanta^{a,b} and Ketan M. Patel^a

^a*Theoretical Physics Division, Physical Research Laboratory,
Navarangpura, Ahmedabad-380009, India*

^b*Indian Institute of Technology Gandhinagar, Palaj-382055, India*

E-mail: gurucharan@prl.res.in, ketan.hep@gmail.com

ABSTRACT: A mechanism for the masses of third, second, and first generation charged fermions at the tree, 1-loop, and 2-loop levels, respectively, is proposed. The fermionic self-energy corrections that lead to this arrangement are induced through heavy vector bosons of a new gauged flavour symmetry group G_F . It is shown that a single Abelian group suffices as G_F . Moreover, the gauge charges are optimized to result in relatively smaller flavour violations in processes involving the first and second generation fermions. The scheme is explicitly implemented on the Standard Model fermions in an anomaly-free manner and is shown to be viable with observed charged fermion masses and quark mixings. Constraints from flavour violations dictate the lower limit on the new physics scale in these types of frameworks. Through optimal flavour violation, it is shown that nearly two orders of magnitude improvement can be achieved on the lower limit, leading to the new physics scale $\geq 10^3$ TeV in this case. Further improvements are possible at the cost of the down quark mass deviating more than 3σ from its value extracted from lattice calculations. Options for inducing tiny masses for light neutrinos are also discussed.

Contents

1	Introduction	1
2	The framework	3
2.1	At tree level	3
2.2	At 1-loop	5
2.3	At 2-loop	7
3	Symmetry deconstruction	9
4	An explicit example of gauge charges	11
5	Integration with the standard model	13
5.1	Implementation	13
5.2	Test of viability	15
6	Phenomenological constraints	18
6.1	Meson-antimeson oscillation	19
6.2	μ to e conversion	22
6.3	$l_i \rightarrow 3l_j$ and $l_i \rightarrow l_j \gamma$	22
7	Neutrino masses	24
7.1	Majorana option	24
7.2	Dirac option	25
8	Summary and further issues	25
A	On the origin of the gauge charges	27
B	Scalar sector	29
C	Details of numerical analysis	30

1 Introduction

The numerous and varied magnitudes of Yukawa couplings have been a perplexing and embarrassing feature of the Standard Model since its inception. Although technically natural, these couplings seem like an ad hoc arrangement to account for the observed flavours, their interchanging interactions, and their masses. It is desirable to have a mechanism that renders at least some of these parameters calculable. Radiative induction is one such possibility, in which some of these couplings are absent at the leading order in perturbation

theory and are generated through loops [1, 2]. This aligns with the observed mass pattern, as the mass hierarchies between two subsequent generations are roughly of the order of the loop suppression factor, $(4\pi^2)^{-1}$.

What could be a minimal setup based on the radiative mass generation mechanism leading to a realistic flavour spectrum? Two requirements guide the efforts to answer this question. Firstly, the framework must lead to accidentally vanishing masses (or corresponding Yukawa couplings) for some generations at the leading order. Secondly, it must possess suitable interactions that induce their non-zero values through quantum corrections. It is straightforward to see that the Standard Model (SM) by itself is not sufficient to enable this. Even if the first n generations ($n \leq 3$) are arranged to be massless by some means, the full action possesses a perturbative global $U(n)^5$ symmetry that prevents the generation of masses for these fermions at higher orders. This was realized in the very early attempts [2–7] and highlighted the need for new interactions violating such a symmetry. Scenarios extending the SM based on new interactions, being mainly of Yukawa type [8–35] or gauge type [36–41] have been proposed. It has been observed that the latter typically provides a more concise and economical alternative from the perspective of overall calculability and predictivity. An extreme example of this is a framework proposed in [38], in which the ambitious implementation turns out to be so predictive that it is discarded by the observed masses and mixing parameters of the charged fermions.

The realistic gauged extensions offering radiative masses for the first and second-generation fermions have been recently worked out in [40, 41]. The symmetry groups investigated as gauged flavour symmetries are abelian $G_F = U(1) \times U(1)$ [40] and non-abelian $G_F = SU(3)$ [41]. Two noteworthy outcomes common to these investigations are: (a) both the second and first generations receive non-zero masses at 1-loop itself, and their intergenerational mass hierarchy can be attributed to the gauge boson mass ordering; and (b) they are compelled to possess $\mathcal{O}(1)$ flavour violating couplings, forcing the new gauge bosons’ masses $\sim 10^8$ GeV or heavier. Both these features primarily depend on the structure of G_F . For example, the choices of G_F in [40, 41] lead to more or less universal values of flavour changing neutral current couplings, namely Q_{ij} , between the i^{th} and j^{th} generations. On the other hand, the present experimental limits from quark and lepton flavour violations are more stringent in the 1-2 sector than in the 2-3 or 1-3 sectors. This suggests that it would be desirable to have $|Q_{12}| < |Q_{23}|, |Q_{13}|$ to somewhat relax the lower limit mentioned in point (b) above. This has phenomenological and technical advantages in terms of observability and naturalness, respectively.

Given the points mentioned above, natural questions arise: Is there a choice of G_F that induces the masses of only the second generation at one loop and the first generation at two loops? Can it accommodate flavour violation in an optimal amount such that the bound on the new gauge boson can be lowered further? The present work attempts to investigate these questions systematically. We begin with the simplest choice $G_F = U(1)$, as it extends the SM with only one gauge boson and obtains the conditions for the charges of the three generations of fermions under this symmetry, such that they obtain masses at successive orders in perturbation theory. In this way, an interesting correlation is found between the loop-induced first-generation mass and flavour violation in the 1-2 sector, such that the

latter vanishes completely in the limit of a massless first generation. By incorporating this mechanism for the SM fermions, the correlation is then exploited to achieve the optimal level of flavor violation while remaining consistent with the observed masses of the first-generation fermions in particular. The viable implementation requires a vectorlike pair of fermions for each charged fermion sector, along with multiple scalars carrying distinct charges under the $U(1)_F$ symmetry.

We begin with a toy framework in the next section and discuss conditions under which $G_F = U(1)_F$ can lead to masses for different generations at different orders in perturbation theory. Section 3 discusses an interplay between the loop-induced masses and flavour changing couplings at each order. In section 4, we provide an explicit example of $U(1)_F$ charges demonstrating these features. The framework is then implemented in the standard model in a phenomenologically viable manner in section 5 and constraints arising mainly from flavour violations are discussed in section 6. We also discuss possibilities to accommodate massive neutrinos within this framework in section 7 before concluding in section 8.

2 The framework

We first describe a mechanism leading to the third, second and first-generation fermion masses at tree, 1-loop and 2-loop levels, respectively, using a general framework. Consider three generations ($i = 1, 2, 3$) of chiral fermions f'_{Li} and f'_{Ri} charged under a local flavour-dependent $U(1)_F$ symmetry with charges q_{Li} and q_{Ri} , respectively. Additionally, consider a pair of vectorlike fermions, namely $F'_{L,R}$, neutral under the $U(1)_F$. Under a chiral gauge symmetry like an electroweak symmetry of the SM, f'_{Li} and f'_{Ri} are to transform differently while F'_L and F'_R are to transform identically. Only the vectorlike fermion has a symmetry-preserving mass.

2.1 At tree level

Once the chiral and $U(1)_F$ symmetries are broken, the fermion mass Lagrangian is assumed to take the following form at the leading order:

$$\begin{aligned} -\mathcal{L}_m &= \mu_{Li} \bar{f}'_{Li} F'_R + \mu_{Ri} \bar{F}'_L f'_{Ri} + m_F \bar{F}'_L F'_R + \text{h.c.}, \\ &\equiv \bar{f}'_{L\alpha} \mathcal{M}_{\alpha\beta}^{(0)} f'_{R\beta} + \text{h.c.}, \end{aligned} \quad (2.1)$$

with $f'_{L(R)4} = F'_{L(R)}$ and $\alpha = i, 4$. The 4×4 matrix $\mathcal{M}^{(0)}$ is given by

$$\mathcal{M}^{(0)} = \begin{pmatrix} 0_{3 \times 3} & (\mu_L)_{3 \times 1} \\ (\mu_R)_{1 \times 3} & m_F \end{pmatrix}, \quad (2.2)$$

with $\mu_L = (\mu_{L1}, \mu_{L2}, \mu_{L3})^T$ and $\mu_R = (\mu_{R1}, \mu_{R2}, \mu_{R3})$. The specific form of interactions in \mathcal{L}_m can be arranged by promoting $\mu_{L,R}$ as spurions and assigning them appropriate charges under the full symmetry of the theory. Both μ_L and μ_R break $U(1)_F$, while at least one of them also breaks the chiral symmetry depending on the choice of the gauge charges of

$F'_{L,R}$. The structure of the tree-level mass matrix, eq. (2.2), closely resembles the form proposed in the context of the universal seesaw mechanism [42–44].

In the physical basis, obtained by $f_{L,R} = \mathcal{U}_{L,R}^{(0)\dagger} f'_{L,R}$, one finds that only one of the chiral generation obtains non-vanishing mass due to the specific structure of $\mathcal{M}^{(0)}$. The bi-unitary diagonalisation leads to

$$\mathcal{U}_L^{(0)\dagger} \mathcal{M}^{(0)} \mathcal{U}_R^{(0)} \equiv \mathcal{D}^{(0)} = \text{Diag.} \left(0, 0, m_3^{(0)}, m_4^{(0)} \right). \quad (2.3)$$

An analytical simplification is possible in the so-called seesaw approximation, $\mu_{L,R} \ll m_F$. The unitary matrices can be expressed as

$$\mathcal{U}_{L,R}^{(0)} = \begin{pmatrix} U_{L,R}^{(0)} & -\rho_{L,R}^{(0)} \\ \rho_{L,R}^{(0)\dagger} U_{L,R}^{(0)} & 1 \end{pmatrix} + \mathcal{O}(\rho^2), \quad (2.4)$$

where

$$\rho_L^{(0)} = -\frac{1}{m_F} \mu_L, \quad \rho_R^{(0)\dagger} = -\frac{1}{m_F} \mu_R, \quad (2.5)$$

are three-dimensional column and row vectors, respectively. $U_{L,R}^{(0)}$ are 3×3 unitary matrices defined from

$$U_L^{(0)\dagger} M^{(0)} U_R^{(0)} = \text{Diag.} \left(0, 0, m_3^{(0)} \right). \quad (2.6)$$

Here, $M^{(0)}$ is an effective 3×3 matrix obtained by integrating out the heavy vectorlike fermion pair. Explicitly,

$$M_{ij}^{(0)} = -\frac{1}{m_F} \mu_{Li} \mu_{Rj}. \quad (2.7)$$

As can be seen, $M^{(0)}$ is essentially a product of two vectors and, therefore, is a rank-1 matrix.

The simple form of $M^{(0)}$ allows one to determine the $U_{L,R}^{(0)}$ analytically. This can be obtained by finding the eigenvector corresponding to the only non-vanishing eigenvalue of $M^{(0)}$ and determining the other two eigenvectors from orthogonality. We find

$$U_L^{(0)} = \begin{pmatrix} -\frac{\mu_{L2}^*}{\sqrt{N_1}} & -\frac{\mu_{L1}\mu_{L3}^*}{\sqrt{N_2}} & \frac{\mu_{L1}}{\sqrt{N_3}} \\ \frac{\mu_{L1}^*}{\sqrt{N_1}} & -\frac{\mu_{L2}\mu_{L3}^*}{\sqrt{N_2}} & \frac{\mu_{L2}}{\sqrt{N_3}} \\ 0 & \frac{|\mu_{L1}|^2 + |\mu_{L2}|^2}{\sqrt{N_2}} & \frac{\mu_{L3}}{\sqrt{N_3}} \end{pmatrix} V_L^{[12]}, \quad (2.8)$$

where $N_{1,2,3}$ are normalization constants that can be determined by normalizing each of the three columns. $V_L^{[12]}$ represents an arbitrary unitary rotation in 1-2 plane, which remain undetermined due to degeneracy among the first two masses. A similar expression for $U_R^{(0)}$ holds with replacement $\mu_L \rightarrow \mu_R^*$.

In the physical basis, the $U(1)_F$ gauge interactions are given by

$$-\mathcal{L}_X = g_X X_\mu \left((\mathcal{Q}_L^{(0)})_{\alpha\beta} \bar{f}_{L\alpha} \gamma^\mu f_{L\beta} + (\mathcal{Q}_R^{(0)})_{\alpha\beta} \bar{f}_{R\alpha} \gamma^\mu f_{R\beta} \right), \quad (2.9)$$

where

$$\mathcal{Q}_{L,R}^{(0)} = \mathcal{U}_{L,R}^{(0)\dagger} \begin{pmatrix} q_{L,R} & 0 \\ 0 & 0 \end{pmatrix} \mathcal{U}_{L,R}^{(0)}, \quad (2.10)$$

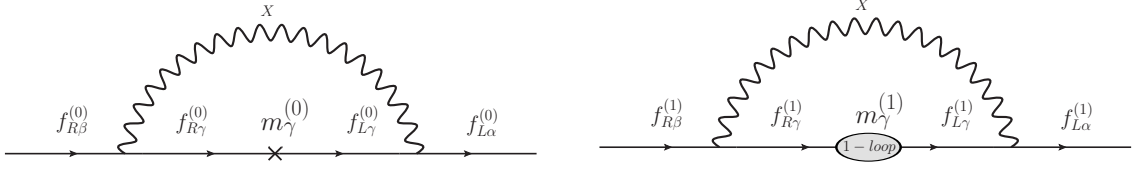


Figure 1. Loop diagrams that generate the masses of second-generation fermions (left panel) and first-generation fermions (right panel).

and

$$q_L = \text{Diag.} (q_{L1}, q_{L2}, q_{L3}) , \quad q_R = \text{Diag.} (q_{R1}, q_{R2}, q_{R3}) . \quad (2.11)$$

For flavour non-universal $q_{L,R}$, the gauge interactions are not flavour diagonal in the physical basis. This plays a pivotal role in inducing the masses of the remaining fermions at higher orders in perturbation theory.

2.2 At 1-loop

The 1-loop corrected fermion mass matrix can be parametrized as

$$\mathcal{M}^{(1)} = \mathcal{M}^{(0)} + \delta\mathcal{M}^{(0)} , \quad (2.12)$$

where

$$\delta\mathcal{M}^{(0)} = \mathcal{U}_L^{(0)} \sigma^{(0)} \mathcal{U}_R^{(0)\dagger} , \quad (2.13)$$

and $\sigma^{(0)}$ captures contributions from the 1-loop diagrams involving fermions and the X -gauge boson in the loop, see the left panel in Fig. 1. It is evaluated as (see for example [40])

$$\sigma_{\alpha\beta}^{(0)} = \frac{g_X^2}{4\pi^2} \sum_{\gamma} (\mathcal{Q}_L^{(0)})_{\alpha\gamma} (\mathcal{Q}_R^{(0)})_{\gamma\beta} m_{\gamma}^{(0)} B_0[M_X, m_{\gamma}^{(0)}] . \quad (2.14)$$

Here,

$$B_0[m_a, m_b] = \Delta_{\epsilon} + 1 - \frac{m_a^2 \ln \frac{m_a^2}{Q^2} - m_b^2 \ln \frac{m_b^2}{Q^2}}{m_a^2 - m_b^2} , \quad (2.15)$$

is a loop integration function evaluated in the dimensional regularization scheme at the renormalization scale Q , and

$$\Delta_{\epsilon} = \frac{2}{\epsilon} - \gamma_E + \ln 4\pi . \quad (2.16)$$

Using eqs. (2.4,2.5,2.6) in (2.13), it is straightforward to show that [40]

$$\delta\mathcal{M}_{ij}^{(0)} \equiv \delta M_{ij}^{(0)} \simeq \frac{g_X^2}{4\pi^2} q_{Li} q_{Rj} M_{ij}^{(0)} \left(B_0[M_X, m_3^{(0)}] - B_0[M_X, m_4^{(0)}] \right) , \quad (2.17)$$

and $\delta\mathcal{M}_{\alpha 4}^{(0)} = \delta\mathcal{M}_{4\alpha}^{(0)} = 0$. The vanishing fourth row and column of $\delta\mathcal{M}_{\alpha\beta}^{(0)}$ are due to the fact that the vectorlike fermions are chosen neutral under $U(1)_F$. The resulting $\mathcal{M}^{(1)}$, therefore, can be written as

$$\mathcal{M}^{(1)} = \begin{pmatrix} (\delta M^{(0)})_{3 \times 3} & \mu_L \\ \mu_R & m_F \end{pmatrix} . \quad (2.18)$$

The diagonalization of $\mathcal{M}^{(1)}$ leads to

$$\mathcal{U}_L^{(1)\dagger} \mathcal{M}^{(1)} \mathcal{U}_R^{(1)} \equiv \mathcal{D}^{(1)} = \text{Diag.} \left(0, m_2^{(1)}, m_3^{(1)}, m_4^{(1)} \right). \quad (2.19)$$

Here, $m_i^{(n)}$ is a mass of i^{th} fermion at n^{th} order. Interestingly, we find $m_1^{(1)} = 0$ and only the second generation mass is induced at the 1-loop level. This is demonstrated below.

In the seesaw limit, the unitary matrices block diagonalizing $\mathcal{M}^{(1)}$ given in eq. (2.18) can be approximated as

$$\mathcal{U}_{L,R}^{(1)} \approx \begin{pmatrix} U_{L,R}^{(1)} & -\rho_{L,R}^{(1)} \\ \rho_{L,R}^{(1)\dagger} U_{L,R}^{(1)} & 1 \end{pmatrix}, \quad (2.20)$$

with $\rho_{L,R}^{(1)} = \rho_{L,R}^{(0)}$. Substituting the above in eq. (2.19), one finds the effective 1-loop corrected 3×3 mass matrix

$$M_{ij}^{(1)} = M_{ij}^{(0)} + \delta M_{ij}^{(0)}, \quad (2.21)$$

such that

$$U_L^{(1)\dagger} M^{(1)} U_R^{(1)} = \text{Diag.} \left(0, m_2^{(1)}, m_3^{(1)} \right). \quad (2.22)$$

It can be noticed that the terms proportional to Δ_ϵ in $\delta M_{ij}^{(0)}$ cancel, rendering the loop-induced mass finite and calculable.

We now show that $M^{(1)}$ always leads to one massless state. Substituting eq. (2.17) in (2.21), it can be simplified to

$$M_{ij}^{(1)} = M_{ij}^{(0)} (1 + C q_{Li} q_{Rj}), \quad (2.23)$$

where $C = \frac{g_X^2}{4\pi^2} (B_0[M_X, m_3^{(0)}] - B_0[M_X, m_4^{(0)}])$. It can then be seen that one of the columns of $M^{(1)}$ is not independent. For example,

$$M_{i1}^{(1)} = \frac{q_{R1} - q_{R3}}{q_{R2} - q_{R3}} \frac{\mu_{R1}}{\mu_{R2}} M_{i2}^{(1)} + \frac{q_{R2} - q_{R1}}{q_{R2} - q_{R3}} \frac{\mu_{R1}}{\mu_{R3}} M_{i3}^{(1)}, \quad (2.24)$$

for $i = 1, 2, 3$. A similar relation also holds between the rows of $M^{(1)}$ with q_R and μ_R replaced by q_L and μ_L , respectively. This implies, for the most general choices of q_R and q_L , that the 1-loop corrected effective mass matrix is of rank-2 and, therefore, one of the states remains massless. In case of the degenerate $q_{L,R}$, $M_{ij}^{(1)}$ remains proportional to $M_{ij}^{(0)}$ leading to only one massive state as expected.

Although obtaining analytical expressions for $U_{L,R}^{(1)}$ can be a complicated exercise, the first columns of $U_{L,R}^{(1)}$ can be derived rather easily. We carry out this by finding the eigenvector corresponding to the vanishing eigenvalue of $M^{(1)} M^{(1)\dagger}$ and $M^{(1)\dagger} M^{(1)}$. The former gives the first column of $U_L^{(1)}$ while the latter gives the same of $U_R^{(1)}$. We find,

$$\begin{pmatrix} U_{L11}^{(1)} \\ U_{L21}^{(1)} \\ U_{L31}^{(1)} \end{pmatrix} = \frac{1}{\sqrt{N}} \begin{pmatrix} 1 \\ \frac{\mu_{L1}^*}{\mu_{L2}^*} \frac{q_{L3} - q_{L1}}{q_{L2} - q_{L1}} \\ -\frac{\mu_{L1}^*}{\mu_{L3}^*} \frac{q_{L2} - q_{L1}}{q_{L2} - q_{L3}} \end{pmatrix}. \quad (2.25)$$

Similar expression with a replacement $L \rightarrow R$ holds for $U_R^{(1)}$. As can be seen, the massless state is a non-trivial combination of all three fermion flavours in general and, therefore, can pick up a mass at a higher order in perturbation theory in a similar way the second-generation mass is induced at 1-loop.

2.3 At 2-loop

Repeating the analysis carried out in the last subsection, we now estimate the first generation mass which gets induced through the next order correction to $\mathcal{M}^{(1)}$. It is captured by the diagram shown in the right panel of Fig. 1. Such a correction can be parametrized as

$$\mathcal{M}^{(2)} = \mathcal{M}^{(1)} + \delta\mathcal{M}^{(1)}, \quad (2.26)$$

with

$$\delta\mathcal{M}^{(1)} = \mathcal{U}_L^{(1)} \sigma^{(1)} \mathcal{U}_R^{(1)\dagger}, \quad (2.27)$$

and $\sigma^{(1)}$ is given by an expression similar to eq. (2.14). Explicitly,

$$\sigma_{\alpha\beta}^{(1)} = \frac{g_X^2}{4\pi^2} \sum_{\gamma} (\mathcal{Q}_L^{(1)})_{\alpha\gamma} (\mathcal{Q}_R^{(1)})_{\gamma\beta} m_{\gamma}^{(1)} B_0[M_X, m_{\gamma}^{(1)}], \quad (2.28)$$

where

$$\mathcal{Q}_{L,R}^{(1)} = \mathcal{U}_{L,R}^{(1)\dagger} \begin{pmatrix} q_{L,R} & 0 \\ 0 & 0 \end{pmatrix} \mathcal{U}_{L,R}^{(1)}, \quad (2.29)$$

is the charge matrix in the new physical basis obtained after 1-loop.

Again, one finds $\delta\mathcal{M}_{\alpha 4}^{(1)} = \delta\mathcal{M}_{4\alpha}^{(1)} = 0$ for the same reason mentioned previously in the context of $\delta\mathcal{M}^{(0)}$. The correction to 3×3 upper left block is explicitly computed as

$$\delta\mathcal{M}_{ij}^{(1)} = \frac{g_X^2}{4\pi^2} q_{Li} q_{Rj} \left(\mathcal{U}_L^{(1)} \right)_{i\gamma} \left(\mathcal{U}_R^{(1)} \right)_{j\gamma}^* m_{\gamma}^{(1)} B_0[M_X, m_{\gamma}^{(1)}]. \quad (2.30)$$

Altogether, $\mathcal{M}^{(2)}$ is given by

$$\mathcal{M}^{(2)} = \begin{pmatrix} (\delta\mathcal{M}^{(1)})_{3 \times 3} & \mu_L \\ \mu_R & m_F \end{pmatrix}, \quad (2.31)$$

with

$$\delta\mathcal{M}_{ij}^{(1)} = \delta M_{ij}^{(0)} + \delta\mathcal{M}_{ij}^{(1)}. \quad (2.32)$$

Further simplification can be achieved in the seesaw approximation. Substituting eq. (2.20) in eq. (2.30) and after some straightforward algebraic simplification, we find

$$\delta\mathcal{M}_{ij}^{(1)} = \frac{g_X^2}{4\pi^2} q_{Li} q_{Rj} \left(\sum_{k=2,3} (U_L^{(1)})_{ik} (U_R^{(1)})_{jk}^* m_k^{(1)} B_0[M_X, m_k^{(1)}] - M_{ij}^{(0)} B_0[M_X, m_F] \right). \quad (2.33)$$

This leads to

$$\begin{aligned}\delta M_{ij}^{(1)} &= \frac{g_X^2}{4\pi^2} q_{Li} q_{Rj} \left(M_{ij}^{(0)} (B_0[M_X, m_3^{(0)}] - 2B_0[M_X, m_F]) \right. \\ &\quad \left. + \sum_{k=2,3} (U_L^{(1)})_{ik} (U_R^{(1)})_{jk}^* m_k^{(1)} B_0[M_X, m_k^{(1)}] \right),\end{aligned}\quad (2.34)$$

for the 3×3 matrix appearing in $\mathcal{M}^{(2)}$.

The diagonalization of $\mathcal{M}^{(2)}$ proceeds as

$$\mathcal{U}_L^{(2)\dagger} \mathcal{M}^{(2)} \mathcal{U}_R^{(2)} \equiv \mathcal{D}^{(2)} = \text{Diag.} \left(m_1^{(2)}, m_2^{(2)}, m_3^{(2)}, m_4^{(2)} \right), \quad (2.35)$$

leading to two-loop induced non-zero mass for the lightest fermion. As before the unitary matrices can be expressed as

$$\mathcal{U}_{L,R}^{(2)} \approx \begin{pmatrix} U_{L,R}^{(2)} & -\rho_{L,R}^{(2)} \\ \rho_{L,R}^{(2)\dagger} U_{L,R}^{(2)} & 1 \end{pmatrix}. \quad (2.36)$$

The form of $\mathcal{M}^{(2)}$ in eq. (2.31) implies $\rho_{L,R}^{(1)} = \rho_{L,R}^{(0)}$. Using the above in eq. (2.35), the effective 3×3 mass matrix at 2-loop is obtained as

$$M_{ij}^{(2)} = M_{ij}^{(0)} + \delta M_{ij}^{(1)}, \quad (2.37)$$

leading to

$$U_L^{(2)\dagger} M^{(2)} U_R^{(2)} = \text{Diag.} \left(m_1^{(2)}, m_2^{(2)}, m_3^{(2)} \right). \quad (2.38)$$

From eqs. (2.34, 2.37) and some algebraic simplification using eq. (2.22), we finally obtain the following effective fermion mass matrix:

$$\begin{aligned}M_{ij}^{(2)} &= M_{ij}^{(0)} \left(1 + \frac{g_X^2}{4\pi^2} q_{Li} q_{Rj} (B_0[M_X, m_3^{(1)}] - B_0[M_X, m_F]) \right) \\ &\quad + \delta M_{ij}^{(0)} \left(1 + \frac{g_X^2}{4\pi^2} q_{Li} q_{Rj} B_0[M_X, m_3^{(1)}] \right) \\ &\quad + \frac{g_X^2}{4\pi^2} q_{Li} q_{Rj} (U_L^{(1)})_{i2} (U_R^{(1)})_{j2}^* m_2^{(1)} (B_0[M_X, m_2^{(1)}] - B_0[M_X, m_3^{(1)}]).\end{aligned}\quad (2.39)$$

The first term in the above is a usual tree-level contribution. The second and third terms parametrize the next-to-leading order contribution. These terms are proportional to $q_{Li} q_{Rj} M_{ij}^{(0)}$. They, along with the tree-level contribution, lead to only two non-vanishing masses. The next-to-next-to-leading order effects arise from the fourth and fifth terms in eq. (2.39) which gives rise to first-generation mass.

The singular part of $M^{(2)}$, as can be read from eq. (2.39), is given by

$$\text{Div.} \left(M_{ij}^{(2)} \right) \propto q_{Li} q_{Rj} \delta M_{ij}^{(0)} \propto q_{Li}^2 q_{Rj}^2 \left(U_L^{(0)} \right)_{i3} \left(U_R^{(0)} \right)_{j3}^* m_3^{(0)}. \quad (2.40)$$

This contribution is of rank-1 and proportional to $m_3^{(0)}$. The divergent part can be removed through renormalizing $m_3^{(0)}$ as the latter is present as a parameter in the theory at tree level. The contribution to the first and second-generation masses arising from eq. (2.39) is, therefore, finite and calculable.

3 Symmetry deconstruction

It is insightful to understand how the assumed structure of the mass Lagrangian and gauge interactions lead to the masses for three generations of chiral fermions at successive orders in perturbation theory by inspecting the associated symmetries. As we show in this section, this helps in finding out the exact nature of the gauge interactions and the parameters in the mass Lagrangian which can lead to desired flavour spectrum.

First, in the absence of \mathcal{L}_m and \mathcal{L}_X , the kinetic terms (along with any other flavour universal gauge interactions such as the ones present in the SM) are invariant under a global $U(3)_L \times U(3)_R$ symmetry. Nonvanishing μ_L and μ_R break this symmetry as it can be seen from \mathcal{L}_m in eq. (2.1). However, one can choose an appropriate $U(3)_{L,R}$ rotations in order to bring $\mu_{L,R}$ in the form $(0, 0, \times)$ where “ \times ” denotes some nonzero number. Therefore, the mass terms in eq. (2.1) leads to

$$U(3)_L \times U(3)_R \xrightarrow{\mu_L \neq 0, \mu_R \neq 0} U(2)_L \times U(2)_R. \quad (3.1)$$

It is this accidental $U(2)_L \times U(2)_R$ symmetry which gives rise to two massless states, identified as the first and second-generation fermions. In the physical basis, $f_{L,R} = \mathcal{U}_{L,R}^{(0)\dagger} f'_{L,R}$, this symmetry of \mathcal{L}_m can be seen more easily.

Next, if the full theory is invariant under this $U(2)_L \times U(2)_R$ then the nonzero masses for the lighter generations of fermions cannot be generated at any order in perturbation theory. In the present framework, breaking of this symmetry is achieved through the gauge interaction Lagrangian \mathcal{L}_X given in eq. (2.9). The breaking¹ of $U(2)_L \times U(2)_R$ appears in the mass Lagrangian at 1-loop. The corrected mass matrix $M_{ij}^{(1)}$, however, possesses again an accidental $U(1)_L \times U(1)_R$ subgroup of the original symmetry,

$$U(2)_L \times U(2)_R \xrightarrow{\text{at 1-loop}} U(1)_L \times U(1)_R, \quad (3.2)$$

leading to a massless state. Again, this symmetry is easier to express in the physical basis. It is defined by the transformations,

$$f_{L1} \rightarrow e^{i\alpha_L} f_{L1}, \quad f_{R1} \rightarrow e^{i\alpha_R} f_{R1}. \quad (3.3)$$

Subsequently, to give rise to non-vanishing mass for the first generation at higher loops involving X -boson, this symmetry must be broken in \mathcal{L}_X . In the new physical basis after 1-loop correction, the relevant charge matrix is:

$$Q_{L,R}^{(1)} = U_{L,R}^{(1)\dagger} q_{L,R} U_{L,R}^{(1)}. \quad (3.4)$$

Invariance of gauge interaction under transformations (3.3) would imply $\left(Q_{L,R}^{(1)}\right)_{12} = \left(Q_{L,R}^{(1)}\right)_{13} = 0$. Non-vanishing $\left(Q_{L,R}^{(1)}\right)_{12,13}$, therefore, are required to generate first-generation mass at

¹Only for specific choices of $q_{L,R}$ leading to $Q_{L,R}^{(0)} = U_{L,R}^{(0)\dagger} q_{L,R} U_{L,R}^{(0)} = \text{Diag.}(q, q, q')$, the gauge interactions in \mathcal{L}_X do not break $U(2)_L \times U(2)_R$ symmetry. Here, $Q_{L,R}^{(0)}$ is upper-left 3×3 block of the matrix $Q_{L,R}^{(0)}$ given in eq. (2.10).

2-loop. Computing explicitly $Q_{L,R}^{(1)}$, we find

$$\begin{aligned} \left(Q_L^{(1)}\right)_{12} &= (q_{L3} - q_{L1}) \left(U_L^{(1)}\right)_{31}^* \left(U_L^{(1)}\right)_{32} + (q_{L2} - q_{L1}) \left(U_L^{(1)}\right)_{21}^* \left(U_L^{(1)}\right)_{22}, \\ &= \frac{(q_{L2} - q_{L1})(q_{L3} - q_{L1})}{\sqrt{N}(q_{L3} - q_{L2})} \left(\frac{\mu_{L1}}{\mu_{L3}} \left(U_L^{(1)}\right)_{32} - \frac{\mu_{L1}}{\mu_{L2}} \left(U_L^{(1)}\right)_{22} \right). \end{aligned} \quad (3.5)$$

Here, the first line is obtained using the orthogonality of the columns of $U_L^{(1)}$ while the second line follows from the expression eq. (2.25). Similarly,

$$\left(Q_L^{(1)}\right)_{13} = \frac{(q_{L2} - q_{L1})(q_{L3} - q_{L1})}{\sqrt{N}(q_{L3} - q_{L2})} \left(\frac{\mu_{L1}}{\mu_{L3}} \left(U_L^{(1)}\right)_{33} - \frac{\mu_{L1}}{\mu_{L2}} \left(U_L^{(1)}\right)_{23} \right), \quad (3.6)$$

and

$$\left(Q_L^{(1)}\right)_{23} = (q_{L3} - q_{L2}) \left(U_L^{(1)}\right)_{32}^* \left(U_L^{(1)}\right)_{33} - (q_{L2} - q_{L1}) \left(U_L^{(1)}\right)_{12}^* \left(U_L^{(1)}\right)_{13}. \quad (3.7)$$

Similar expressions can also be obtained for $\left(Q_R^{(1)}\right)_{ij}$ following the steps outlined above.

For $q_{L3} \neq q_{L2}$, it is noted that $(Q_L^{(1)})_{12,13}$ vanish in the limit: $q_{L1} \rightarrow q_{L2}$ or $q_{L1} \rightarrow q_{L3}$ or $\mu_{L1} \rightarrow 0$. Therefore, complete flavour non-degenerate $q_{L,R}$ and non-vanishing $(\mu_{L,R})_1$ are necessary to break the accidental $U(1)_L \times U(1)_R$ symmetry. The breaking of the latter appears at 2-loop and leads to suppressed but non-vanishing mass for the lightest fermion. Hence, at 2-loop,

$$U(1)_L \times U(1)_R \xrightarrow{\text{at 2-loop}} U(1)_{\text{fn}}, \quad (3.8)$$

where $U(1)_{\text{fn}}$ is a global fermion number which remains as an unbroken symmetry at least at the perturbative level in this setup.

Also, it can be noticed from the \mathcal{L}_m that if any of the μ_{Li} or μ_{Ri} is zero, then the corresponding f'_{Li} or f'_{Ri} does not mix with the rest of the fermions. As both the mass Lagrangian and gauge interactions are invariant under a $U(1)_L$ or $U(1)_R$ (under which $f'_{L(R)i} \rightarrow e^{i\theta} f'_{L(R)i}$), such a symmetry remains unbroken by the quantum corrections, leading to a massless fermion at all orders. Therefore, it is necessary to have all μ_{Li} and μ_{Ri} nonvanishing in the present framework.

Two important observations that emerge from the above discussions are:

- Complete non-degeneracy in the flavour charges is necessary to induce the second generation mass at 1-loop and the first generation mass at 2-loop level. In addition, all μ_{Li} and μ_{Ri} are required to be non-vanishing. As a consequence, the flavour changing current mediated through the X -boson is inherently present in the framework.
- Up to 1-loop corrected mass Lagrangian, the strength of flavour changing current in 1-2 and 2-3 sectors, are parametrized by $\left(Q_L^{(1)}\right)_{12}$ and $\left(Q_L^{(1)}\right)_{23}$, respectively. Phenomenologically, it is desired to arrange $\left|\left(Q_L^{(1)}\right)_{12}\right| < \left|\left(Q_L^{(1)}\right)_{23}\right|$, as the experimental constraints from flavour violating processes in 1-2 sector are relatively more severe. As can be seen from eq. (3.5), this can be arranged if

$$|q_{L2} - q_{L1}| \ll |q_{L3} - q_{L2}| \quad \text{or} \quad |q_{L3} - q_{L1}| \ll |q_{L3} - q_{L2}|, \quad (3.9)$$

and

$$|\mu_{L1}| < |\mu_{L2}|, |\mu_{L3}|. \quad (3.10)$$

The same applies to the parameters with $L \rightarrow R$ in the subscripts.

These observations play a decisive role in fixing the exact nature of $U(1)_F$ as we discuss in the next section.

4 An explicit example of gauge charges

We now discuss a possible choice for the flavour-dependent gauge charges and their implications on the loop-induced masses in the toy framework. Without losing much of the freedom in choosing flavour-specific charges, an easy way to ensure that the $U(1)_F$ is non-anomalous is to consider $U(1)_F$ as a vectorlike symmetry, i.e. $q_{Li} = q_{Ri}$ for each i . This choice is sufficient to cancel $[U(1)_F]^3$ and mixed gauge-gravity anomalies. Non-chiral nature of $U(1)_F$ by itself does not forbid the bare mass terms like $\bar{f}'_{Li} f'_{Ri}$ whose presence in \mathcal{L}_m in eq. (2.1) can spoil the radiative mass generation mechanism and, therefore, an additional chiral symmetry may be needed. In the case of the SM, as we show in the next section, the gauge symmetry of the model itself can be utilised to serve this purpose.

Once $q_{Li} = q_{Ri}$ are chosen, one of the three charges can be fixed to a non-zero number without losing the generality. Based on this fact and the points summarized at the end of the previous section, we choose:

$$q_{L1} = q_{R1} = 1 - \epsilon, \quad q_{L2} = q_{R2} = 1 + \epsilon, \quad q_{L3} = q_{R3} = -2, \quad (4.1)$$

with $0 < \epsilon \leq 1$. Also, we have chosen the charges such that $\text{Tr}(q_{L,R}) = 0$. This makes it easier to cancel some of the mixed gauge anomalies when this toy framework is generalised to be integrated with the SM. For $\epsilon \ll 1$, the strength of flavour violation in 1-2 sector can be relatively suppressed as argued in section 3. Explicitly, for this choice, one finds from eqs. (3.5,3.7):

$$\left| \frac{(Q_L^{(1)})_{12}}{(Q_L^{(1)})_{23}} \right| \simeq \frac{2|\epsilon|}{3\sqrt{N}} \left| \frac{\frac{\mu_{L1}}{\mu_{L3}} (U_L^{(1)})_{32} - \frac{\mu_{L1}}{\mu_{L2}} (U_L^{(1)})_{22}}{(U_L^{(1)})_{32}^* (U_L^{(1)})_{33}} \right|. \quad (4.2)$$

When the condition, eq. (3.10), is applied, $|\epsilon| \ll 1$ leads to $\left| (Q_L^{(1)})_{12} \right| \ll \left| (Q_L^{(1)})_{23} \right|$. However, for $\epsilon = 0$, one obtains a massless generation of fermions and therefore ϵ needs to be suitably optimized.

It can be seen that $\epsilon = 1$ reproduces an all-flavour version of the famous $L_\mu - L_\tau$ symmetry which we used for radiative generation of masses previously [40]. Although, its generalisation in terms of charges given in eq. (4.1) looks ad-hoc, it can be shown to arise naturally in the effective theory from $U(1) \times U(1)$ gauge theory with well-defined charges and kinetic mixing. This is explicitly demonstrated in Appendix A. The free parameter ϵ can be associated with the kinetic mixing in this case. We also show that the underlying $U(1) \times U(1)$ symmetries, when combined with a flavour universal abelian symmetry like

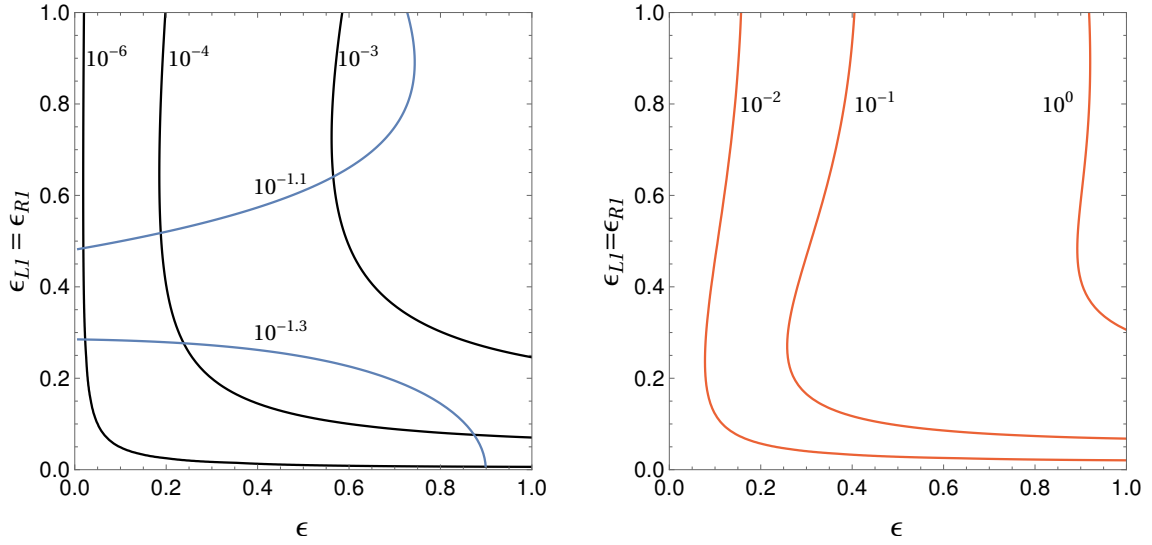


Figure 2. Left panel: contours of $m_1/m_3 = 10^{-6}, 10^{-4}, 10^{-3}$ (black) and $m_2/m_3 = 10^{-1.1}, 10^{-1.3}$ (blue). Right panel: contours of $|Q_{12}^{(2)}|^2 / |Q_{23}^{(2)}|^2 = 10^{-2}, 0.1$ and 1 .

hypercharge, can be recast into $U(1)_1 \times U(1)_2 \times U(1)_3$ such that only one generation of fermions is non-trivially charged under each $U(1)$. Models of this variety have been recently proposed in [45, 46] although not from the perspective of radiative mass mechanism.

To explicitly demonstrate that the choice of gauge charges in eq. (4.1) leads to the desired pattern of fermion masses and flavour violating couplings, we numerically compute the 2-loop corrected mass matrix $M^{(2)}$ from eq. (2.39) for an example set of input parameters. For the latter, we consider $g_X = 0.5$, $M_X = 10$ TeV, $m_F = 10 M_X$, $\mu_L = (\epsilon_{L1}, 0.3, 1) \frac{v}{\sqrt{2}}$, $\mu_R = (\epsilon_{R1}, 0.3, 1)$ TeV, $v = 246$ GeV and $Q = M_Z$. The mass ratios m_1/m_3 , m_2/m_3 for different values of ϵ and $\epsilon_{L1} = \epsilon_{R1} \equiv \epsilon_1$ are displayed in the left panel of Fig. 2. As it is anticipated, m_1/m_3 decreases as ϵ or ϵ_1 become smaller. m_2/m_3 is not very sensitive to ϵ as the hierarchy between m_2 and m_3 is mostly governed by the loop factor. Similarly, the contours of the ratio $|Q_{12}^{(2)}|^2 / |Q_{23}^{(2)}|^2$ are shown in the right panel of Fig. 2.

As it can be seen, $10^{-6} \gtrsim m_1/m_3 \gtrsim 10^{-4}$ typically prefers ϵ in the range 0.05-0.5 for generic values of ϵ_1 . This leads to $|Q_{12}^{(2)}|^2 \lesssim 0.1 |Q_{23}^{(2)}|^2$ as desired. Nevertheless, $|Q_{12}^{(2)}|$ cannot be made arbitrarily small as it requires very small ϵ and ϵ_1 . As discussed in the previous section and also confirmed by Fig. 2, this corresponds to the almost massless first generation. By fixing $\epsilon = \epsilon_1 = 0.2$, we also show the absolute values of three masses and flavour violating couplings $|Q_{ij}^{(n)}|$ in Fig. 3 at n loop. Due to degeneracy between m_1 and m_2 at the leading order, $|Q_{12}^{(0)}|$ is undefined. The latter gets fixed at 1-loop. Fig. 3 shows that the masses and $|Q_{ij}^{(n)}|$ receive only small corrections at the next order and the ordering between them remains unchanged.

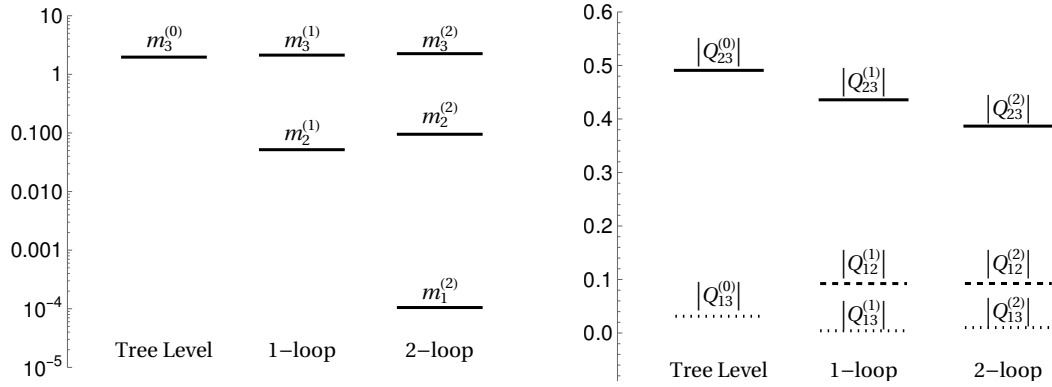


Figure 3. Left panel: Fermion masses at tree, 1-loop and 2-loop level for $\epsilon = \epsilon_{L1} = \epsilon_{R1} = 0.2$ and for the remaining parameters as specified in the text. Right panel: For the same parameters, the magnitudes of $Q_{ij}^{(n)}$.

5 Integration with the standard model

This section discusses the integration of the above scheme with the SM and its viability in reproducing the observed charged fermion spectrum. We continue to work with the gauge charges as displayed in eq. (4.1) and apply them universally to all the SM fermions.

5.1 Implementation

It is straightforward to implement the underlying mechanism for the SM fermions, leading to loop-induced mass hierarchies for the charged fermions. The left chiral fields are generalised to include the electroweak quark and lepton doublets, Q_{Li} and L_{Li} . Similarly, the right chiral SM fields include u_{Ri} , d_{Ri} and e_{Ri} . For the vectorlike fermions in each sector, we choose $U_{L,R}$, $D_{L,R}$ and $E_{L,R}$ which under the SM gauge symmetry transform in the same way as u_{Ri} , d_{Ri} and e_{Ri} , respectively. The role of μ_{Li} is played by three pairs of electroweak doublets scalars H_{ui} and H_{di} while terms proportional to μ_{Ri} are to originate from three SM singlet scalars η_i . The three generations of chiral fermions and scalars have flavour non-universal charges identical to the ones mentioned in eq. (4.1). The field content of the model and their charges under the SM and $U(1)_F$ gauge symmetries are summarized in Table 1.

The presence of three generations of ν_R with $U(1)_F$ charges as listed in Table 1 is essential to retain the vector structure of $U(1)_F$ symmetry which, as discussed in the previous section, ensures the cancellation of the cubic $U(1)_F$ and mixed gauge-gravity anomalies. It also implies vanishing $U(1)_Y \times U(1)_F^2$ anomaly. Moreover, the choice $\text{Tr}(q_{L,R}) = 0$ leads to cancellation of anomalies associated with $SU(2)_L^2 \times U(1)_F$ and $U(1)_Y^2 \times U(1)_F$. The field content and gauge charges given in Table 1, therefore, lead to a theoretically consistent framework.

The renormalizable and gauge invariant Yukawa and mass Lagrangian involving the

Fields	$SU(3)_C \times SU(2)_L \times U(1)_Y$	$U(1)_F$
Q_{Li}	$(3, 2, \frac{1}{6})$	$(1 - \epsilon, 1 + \epsilon, -2)$
u_{Ri}	$(3, 1, \frac{2}{3})$	$(1 - \epsilon, 1 + \epsilon, -2)$
d_{Ri}	$(3, 1, -\frac{1}{3})$	$(1 - \epsilon, 1 + \epsilon, -2)$
L_{Li}	$(1, 2, -\frac{1}{2})$	$(1 - \epsilon, 1 + \epsilon, -2)$
e_{Ri}	$(1, 1, -1)$	$(1 - \epsilon, 1 + \epsilon, -2)$
ν_{Ri}	$(1, 1, 0)$	$(1 - \epsilon, 1 + \epsilon, -2)$
$U_{L,R}$	$(3, 1, \frac{2}{3})$	0
$D_{L,R}$	$(3, 1, -\frac{1}{3})$	0
$E_{L,R}$	$(1, 1, -1)$	0
H_{ui}	$(1, 2, -\frac{1}{2})$	$(1 - \epsilon, 1 + \epsilon, -2)$
H_{di}	$(1, 2, \frac{1}{2})$	$(1 - \epsilon, 1 + \epsilon, -2)$
η_i	$(1, 1, 0)$	$(1 - \epsilon, 1 + \epsilon, -2)$

Table 1. List of fields and their flavour-universal SM and flavour-dependent $U(1)_F$ gauge charges.

fermions can be written as

$$\begin{aligned}
-\mathcal{L}_Y = & y_{ui} \bar{Q}_{Li} H_{ui} U_R + y_{di} \bar{Q}_{Li} H_{di} D_R + y_{ei} \bar{L}_{Li} H_{di} E_R \\
& + y'_{ui} \bar{U}_L \eta_i^* u_{Ri} + y'_{di} \bar{D}_L \eta_i^* d_{Ri} + y'_{ei} \bar{E}_L \eta_i^* e_{Ri} \\
& + m_U \bar{U}_L U_R + m_D \bar{D}_L D_R + m_E \bar{E}_L E_R + \text{h.c.} .
\end{aligned} \tag{5.1}$$

As usual, the direct mass term for the three generations of fermions is forbidden by the chiral structure of the SM gauge symmetry even if they are allowed by $U(1)_F$. The non-trivial transformation assigned to the Higgs fields under the new gauge symmetry also forbids the direct Yukawa couplings between the left- and right-chiral fields of the SM. The fermionic current associated with the flavour non-universal gauge interactions, $\mathcal{L}_X = j_X^\mu X_\mu$, is given by

$$j_X^\mu = g_X \left(\sum_{f=Q,L} q_{Li} \bar{f}_{Li} \gamma^\mu f_{Li} + \sum_{f=u,d,e} q_{Ri} \bar{f}_{Ri} \gamma^\mu f_{Ri} \right), \tag{5.2}$$

with the choice of q_{Li} and q_{Ri} as listed in Table 1.

The most general non-vanishing vacuum of η_i breaks the $U(1)_F$ completely. As usual, the electroweak symmetry is to be broken by the $U(1)_{\text{em}}$ preserving vacuum expectation values (VEVs) of H_{ui} , H_{di} which also contribute to the breaking of $U(1)_F$. We parametrize these VEVs as

$$y_{fi} \langle H_{fi} \rangle \equiv \mu_{fi}, \quad y'_{fi} \langle \eta_i^* \rangle \equiv \mu'_{fi}, \tag{5.3}$$

with $f = u, d, e$ and $\langle H_{ei} \rangle = \langle H_{di} \rangle$. The condition $\sum_i (|\langle H_{ui} \rangle|^2 + |\langle H_{di} \rangle|^2) = (246 \text{ GeV})^2$ typically implies that μ_{fi} are at most of the order of the electroweak scale while there is no such restriction on the magnitudes of μ'_{fi} .

It can be seen that the substitution of eq. (5.3) in (5.1) makes the latter take the precise form of the interactions depicted in eq. (2.1). The $\mathcal{M}^{(0)}$ given in eq. (2.2) has

been replicated for $f = u, d, e$ with $\mu_{Li} \rightarrow \mu_{fi}$ and $\mu_{Ri} \rightarrow \mu'_{fi}$. Using the results derived in section 2, one finds the 2-loop corrected effective 3×3 matrix for the charged fermions as

$$\begin{aligned} \left(M_f^{(2)}\right)_{ij} &= \left(M_f^{(0)}\right)_{ij} \left(1 + \frac{g_X^2}{4\pi^2} q_{Li} q_{Rj} (b_0[M_X, m_{f3}^{(1)}] - b_0[M_X, m_F])\right) \\ &+ \left(\delta M_f^{(0)}\right)_{ij} \left(1 + \frac{g_X^2}{4\pi^2} q_{Li} q_{Rj} b_0[M_X, m_{f3}^{(1)}]\right) \\ &+ \frac{g_X^2}{4\pi^2} q_{Li} q_{Rj} (U_{fL}^{(1)})_{i2} (U_{fR}^{(1)})_{j2}^* m_{f2}^{(1)} (b_0[M_X, m_{f2}^{(1)}] - b_0[M_X, m_{f3}^{(1)}]), \end{aligned} \quad (5.4)$$

for $f = u, d, e$. The corresponding mass matrices at the tree-level and one-loop are given by

$$\left(M_f^{(0)}\right)_{ij} = -\frac{1}{m_F} \mu_{fi} \mu'_{fj}, \quad (5.5)$$

and

$$\left(M_f^{(1)}\right)_{ij} = \left(M_f^{(0)}\right)_{ij} (1 + C_f q_{Li} q_{Rj}), \quad (5.6)$$

respectively, with $C_f = \frac{g_X^2}{4\pi^2} (b_0[M_X, m_{f3}^{(0)}] - b_0[M_X, m_F])$.

Eqs. (5.4, 5.5, 5.6) are straightforward generalisation of eqs. (2.39, 2.7, 2.21). $m_{fi}^{(n)}$ appearing in these equations is the i^{th} eigenvalue of $M_f^{(n)}$ and can be computed using the given expressions. Similarly, $U_{fL}^{(1)}$ and $U_{fR}^{(1)}$ can be evaluated from the diagonalisation of $M_f^{(1)}$ following the usual definition, eq. (2.22). b_0 is the finite part of the function B_0 as defined in the $\overline{\text{MS}}$ scheme and is given by

$$b_0[m_a, m_b] = 1 - \frac{m_a^2 \ln \frac{m_a^2}{Q^2} - m_b^2 \ln \frac{m_b^2}{Q^2}}{m_a^2 - m_b^2}. \quad (5.7)$$

In the present model, the scalars can also give rise to radiative correction to the fermions mass matrices through diagrams similar to Fig. 1 with X -boson replaced by the physical scalar fields. However, the form of interactions in eq. (5.1) dictates that these contributions always depend on $H_{u,d}-\eta$ mixing. In turn, they depend on the several new parameters which are otherwise unconstrained and can spoil the calculability and predictivity offered by eq. (5.4). Therefore, it would be desirable to suppress these contributions by assuming small or vanishing $H_{u,d}-\eta$ mixing. In Appendix B, we outline conditions leading to this. In the subsequent analysis, we neglect the scalar-induced contributions and use eq. (5.4) to quantify the quantum corrections to the fermion masses.

5.2 Test of viability

In order to demonstrate that $M_f^{(2)}$ obtained in eq. (5.4) can lead to realistic charged fermion masses for $f = u, d, e$ and the quark mixing parameters, we carry out a numerical analysis following the method developed and described in detail in our previous work [40]. The essential points of the same are outlined in Appendix C for the convenience of the reader.

We set $g_X = 0.5$ and optimize the χ^2 function for several values of ϵ and a few example values of M_X . The remaining 23 parameters are left to be optimized considering some

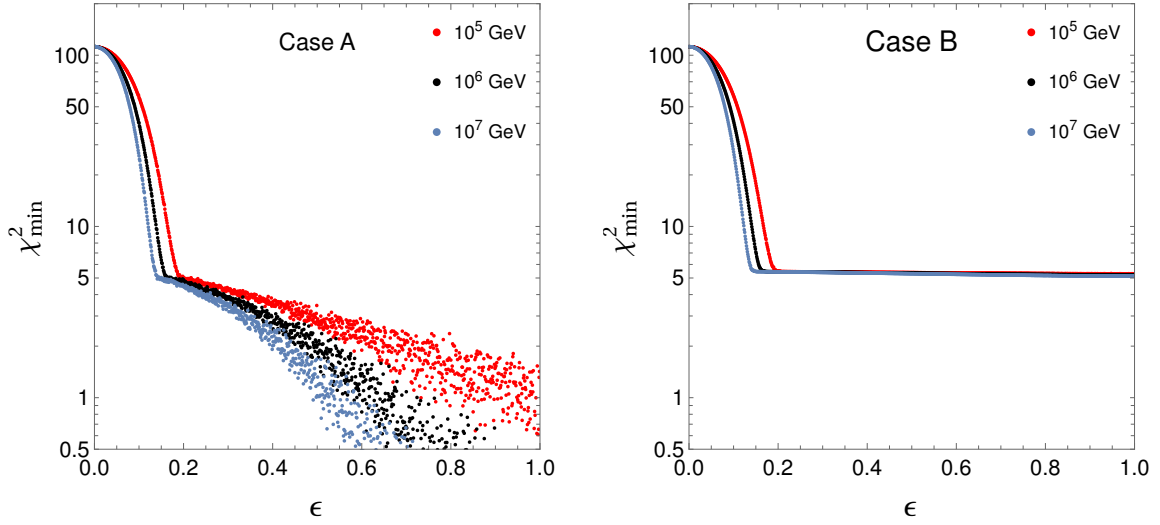


Figure 4. The obtained χ^2_{\min} as a function of ϵ for three sample values of M_X with conditions categorized under case A (left panel) and case B (right panel).

usual constraints, see discussion in Appendix C. The entire exercise is carried out for the following two scenarios:

- Case A: Ordered μ_{fi} and μ'_{fi} , i.e. for $f = u, d, e$, we impose

$$|\mu_{f1}| < |\mu_{f2}| < |\mu_{f3}|, \quad \text{and} \quad |\mu'_{f1}| < |\mu'_{f2}| < |\mu'_{f3}|. \quad (5.8)$$

- Case B: Strongly ordered μ_{di} and μ'_{di} . In this case in addition to the conditions in eq. (5.8), we impose

$$\frac{|\mu_{d1}|}{|\mu_{d2}|} < 0.1, \quad \text{and} \quad \frac{|\mu'_{d1}|}{|\mu'_{d2}|} < 0.1. \quad (5.9)$$

Both these conditions help in achieving phenomenologically favoured ordering in flavour violations as discussed in section 4 and provide a transparent connection between the flavour violation in 1-2 sector and the parameter ϵ . Case B, in particular, points out a parameter space in which the strongest constraints from the K^0 - \bar{K}^0 oscillations can be evaded more effectively, as we show later in the next section.

The results of minimized χ^2 for different values of ϵ and M_X for both the above cases are displayed in Fig. 4. The fits corresponding to $\chi^2_{\min} \leq 9$ can be considered acceptable, as none of the observables is more than 3σ away from its mean value. Keeping this in consideration, the noteworthy observations from Fig. 4 are the following.

- The fits in all cases disfavour $\epsilon < 0.15$. We find that for the smaller values of ϵ , the first-generation masses do not get fitted to their experimentally extracted values within their 3σ ranges. This is in agreement with expectation discussed in section 4.
- In case A, the fit improves with larger values of ϵ . In fact, for $M_X \geq 10^6$ GeV, excellent fits can be achieved corresponding to $\chi^2_{\min} \lesssim 1$ for $\epsilon > 0.5$ implying that all

Observable	O_{exp}	Solution 1		Solution 2	
		O_{th}	Pull	O_{th}	Pull
m_u [MeV]	1.27 ± 0.5	1.26	-0.02	1.27	0
m_c [GeV]	0.619 ± 0.084	0.614	-0.06	0.617	-0.02
m_t [GeV]	171.7 ± 3.0	171.8	0.03	171.7	0
m_d [MeV]	2.90 ± 1.24	0.16	-2.21	0.02	-2.32
m_s [GeV]	0.055 ± 0.016	0.056	0.06	0.055	0
m_b [GeV]	2.89 ± 0.09	2.89	0	2.89	0
m_e [MeV]	0.487 ± 0.049	0.489	0.04	0.487	0
m_μ [GeV]	0.1027 ± 0.0103	0.1025	-0.02	0.1025	-0.02
m_τ [GeV]	1.746 ± 0.174	1.746	0	1.742	-0.02
$ V_{us} $	0.22500 ± 0.00067	0.22499	-0.01	0.22500	0
$ V_{cb} $	0.04182 ± 0.00085	0.04182	0	0.04182	0
$ V_{ub} $	0.00369 ± 0.00011	0.00369	0	0.00369	0
J_{CP}	3.08×10^{-5}	3.08×10^{-5}	0	3.08×10^{-5}	0
χ_{min}^2			4.9		5.4

Table 2. Two benchmark solutions of best-fit from cases A and B, respectively. O_{exp} denote the extrapolated values of the respective observables at the renormalization scale $Q = M_Z$. The reproduced values of the observables at χ_{min}^2 are listed under O_{th} and the corresponding pulls are given which indicates the amount of deviation from the mean O_{exp} value.

the observables can be fitted within their 1σ ranges. Also, improvement in fits for a given ϵ is observed with larger M_X .

- In contrast to the above, $\chi_{\text{min}}^2 < 5$ cannot be achieved for any value of ϵ and M_X in case B. We find that with conditions in eq. (5.9) the mass of the down quark remains 2.3σ away from its central value irrespective of the other parameters.

From the above observations, it is evident that the mechanism can be implemented on the SM in a phenomenologically consistent manner only if $\epsilon > 0.15$. This exact lower limit then implies a finite amount of flavour violation in the 1-2 sector, which we discuss in detail in the next section.

To demonstrate the efficiency of the fits and behaviour of the fitted parameters, we give two explicit benchmark solutions in Table 2. The Solution 1 (S1) falls within case A. Solution 2 (S2) corresponds to strongly ordered μ_{di} and μ'_{di} in case B. They are also chosen with optimized values of ϵ and M_X from the perspective of flavour violation, as will be revealed in the next section. It can be seen that all the observables, except m_d , are fitted excellently. m_d remains more than 2σ away in both the cases. Therefore, future improvements in the uncertainty in m_d can have a significant effect on the viability of these types of solutions.

The values of ϵ and M_X for the chosen benchmark solutions and numerical values of all the remaining 25 real parameters at the minimum of χ^2 are listed in Table 4 in Appendix

C. The most noteworthy aspect of the values of the various parameters in both cases is that all μ_{fi} and μ'_{fi} are spread in the range of only two orders of magnitude at most. This, when interpreted in terms of eq. (5.3), implies that all the fundamental Yukawa couplings can be of $\mathcal{O}(1)$ in this kind of model. Obviously, the hierarchies in the observed masses are then attributed to the very intricate and carefully arranged structure of the theory. It is also noticed that the vectorlike fermions must stay close to the $U(1)_F$ breaking scale. This is to avoid large seesaw suppression in the masses of the third-generation fermions. This is more apparent in the case of top quark mass, which forces $m_U \simeq \mu'_{u3}$. Relatively light m_b and m_τ are arranged through $m_D > \mu'_{d3}$ and $m_E > \mu'_{e3}$, respectively.

6 Phenomenological constraints

The most significant constraint on the new physics in the present setup is expected to come from flavour changing neutral current (FCNC) interactions of the SM fermions. They can arise in three ways: (i) through a direct mediation by X -boson which has flavour changing couplings, (ii) through Z -boson and mixing of the SM fermions with the vectorlike ones, and (iii) through a mediation by neutral scalars. The first is parametrized by eq. (5.2) in the physical basis of the quarks and charged leptons as

$$j_X^\mu = g_X \sum_{f=u,d,e} \left((X_L^f)_{ij} \bar{f}_{Li} \gamma^\mu f_{Lj} + (X_R^f)_{ij} \bar{f}_{Ri} \gamma^\mu f_{Rj} \right), \quad (6.1)$$

with

$$X_{L,R}^f = U_{L,R}^{f\dagger} q_{L,R} U_{L,R}^f, \quad (6.2)$$

and $U_{L,R}^f$ being the 3×3 unitary matrices that diagonalize the corresponding 2-loop corrected $M_f^{(2)}$ given in eq. (5.4) such that $U_L^{f\dagger} M_f^{(2)} U_R^f = \text{Diag.}(m_{f1}^{(2)}, m_{f2}^{(2)}, m_{f3}^{(2)})$.

The current associated with the Z -boson in the physical basis is obtained as

$$j_Z^\mu = -\frac{g}{2 \cos \theta_W} \left(\mathcal{Y}_{\alpha\beta}^u \bar{u}_{L\alpha} \gamma^\mu u_{L\beta} - \mathcal{Y}_{\alpha\beta}^d \bar{d}_{L\alpha} \gamma^\mu d_{L\beta} - \mathcal{Y}_{\alpha\beta}^e \bar{e}_{L\alpha} \gamma^\mu e_{L\beta} - 2 \sin^2 \theta_W J_{\text{em}}^\mu \right), \quad (6.3)$$

where J_{em}^μ is flavour diagonal electromagnetic current. The 4×4 coupling matrices are given by

$$\mathcal{Y}^f = \mathcal{U}_L^{f(2)\dagger} \begin{pmatrix} \mathbf{1}_{3 \times 3} & 0 \\ 0 & 0 \end{pmatrix} \mathcal{U}_L^{f(2)}. \quad (6.4)$$

Using the seesaw expansion, eq. (2.36), one finds

$$\mathcal{Y}_{ij}^f \simeq \delta_{ij} + \mathcal{O}\left(\frac{\mu_f \mu'_f}{m_F^2}\right). \quad (6.5)$$

Apparently, the off-diagonal elements are suppressed by heavy-light mixing. For the values of μ_f and m_F given Table 4, one finds that the FCNCs induced by the Z -boson remain suppressed in comparison to that induced by the X -boson.

Similarly, the flavour changing couplings of the neutral scalars are also found suppressed by the heavy-light mixing. This is demonstrated in detail in Appendix B. Consequently,

if the scalar masses are of $\mathcal{O}(M_X)$, the FCNC's induced by the scalars provide only the sub-leading contributions to the ones mediated by the $U(1)_X$ gauge boson. Therefore, we focus on the current parametrized by eq. (6.1) and derive the constraints on M_X arising from the following most relevant observables.

6.1 Meson-antimeson oscillation

The most stringent limits on quark sector FCNC couplings arise from the neutral meson-antimeson oscillations, namely $M^0-\bar{M}^0$ transitions, where $M = K, B_d, B_s, D$. To evaluate these constraints in the context of the present model, we follow the methodology developed and discussed in detail in our previous work [40]. The effective four-fermion operators obtained by eliminating the X -boson are given by

$$\mathcal{L}_X^{\text{eff}} = -\frac{1}{M_X^2} j_X^\mu j_{X\mu}, \quad (6.6)$$

where j_X^μ is already specified in eq. (6.1). This can be compared with the effective Hamiltonian, $\mathcal{H}_M^{\text{eff}} = \sum_{i=1}^5 C_M^i Q^i + \sum_{i=1}^3 \tilde{C}_M^i \tilde{Q}_i$ that parametrizes $\Delta F = 2$, $M^0-\bar{M}^0$ transitions in terms of the familiar Wilson coefficients [47]. Through this, we can identify the respective Wilson coefficients C_M^i and \tilde{C}_M^i in terms of flavour violating couplings present in the underlying model. At the matching scale $Q = M_X$, we find:

$$\begin{aligned} C_K^1 &= \frac{g_X^2}{M_X^2} \left[(X_L^d)_{12} \right]^2, \quad \tilde{C}_K^1 = \frac{g_X^2}{M_X^2} \left[(X_R^d)_{12} \right]^2, \quad C_K^5 = -4 \frac{g_X^2}{M_X^2} (X_L^d)_{12} (X_R^d)_{12}, \\ C_{B_d}^1 &= \frac{g_X^2}{M_X^2} \left[(X_L^d)_{13} \right]^2, \quad \tilde{C}_{B_d}^1 = \frac{g_X^2}{M_X^2} \left[(X_R^d)_{13} \right]^2, \quad C_{B_d}^5 = -4 \frac{g_X^2}{M_X^2} (X_L^d)_{13} (X_R^d)_{13}, \\ C_{B_s}^1 &= \frac{g_X^2}{M_X^2} \left[(X_L^d)_{23} \right]^2, \quad \tilde{C}_{B_s}^1 = \frac{g_X^2}{M_X^2} \left[(X_R^d)_{23} \right]^2, \quad C_{B_s}^5 = -4 \frac{g_X^2}{M_X^2} (X_L^d)_{23} (X_R^d)_{23}, \\ C_D^1 &= \frac{g_X^2}{M_X^2} [(X_L^u)_{12}]^2, \quad \tilde{C}_D^1 = \frac{g_X^2}{M_X^2} [(X_R^u)_{12}]^2, \quad C_D^5 = -4 \frac{g_X^2}{M_X^2} (X_L^u)_{12} (X_R^u)_{12}. \end{aligned} \quad (6.7)$$

The rest of the C_M^i and \tilde{C}_M^i are vanishing at $Q = M_X$.

Next, all the coefficients are evolved using appropriate renormalization group equations (RGE) from $Q = M_X$ to $Q = 2$ GeV for $K^0-\bar{K}^0$ system [48], to $Q = 4.6$ GeV for $B_{d,s}^0-\bar{B}_{d,s}^0$ system [49], and to $Q = 2.8$ GeV for $D^0-\bar{D}^0$ system [47]. It is seen that the running induces non-vanishing values for C_M^4 while $\tilde{C}_M^{2,3}$ and $C_M^{2,3}$ remain zero. Following this and using the expressions in eqs. (6.2) and (6.7), we numerically compute the values of all the non-vanishing Wilson coefficients at their relevant low-energy scales for each point displayed in Fig. 4. These values are then compared with the present experimental limits obtained by the UTFit collaboration [47].

Among all the C_M^i and \tilde{C}_M^i computed in the present model, we find that the strongest limits on M_X are almost entirely driven by $\text{Re}C_K^{4,5}$. To demonstrate this, we give their values as a function of ϵ for $M_X = 10^6$ and $M_X = 10^7$ GeV in Figs. 5 and 6, respectively.

We also provide these estimations for cases A and B as discussed in the previous section. As it can be verified from both the figures, the flavour constraints can be efficiently evaded

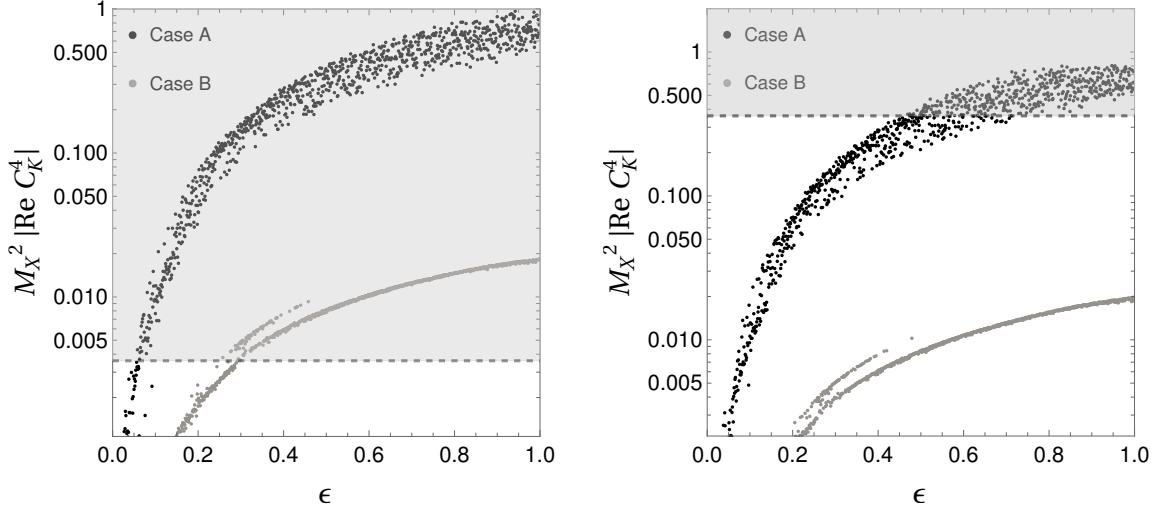


Figure 5. Magnitude of $\text{Re} C_K^4$ computed for the best-fit points for different values of ϵ and for $M_X = 10^6$ GeV (left panel) and $M_X = 10^7$ GeV (right panel). The shaded regions are excluded by the present limits at 95% confidence level.

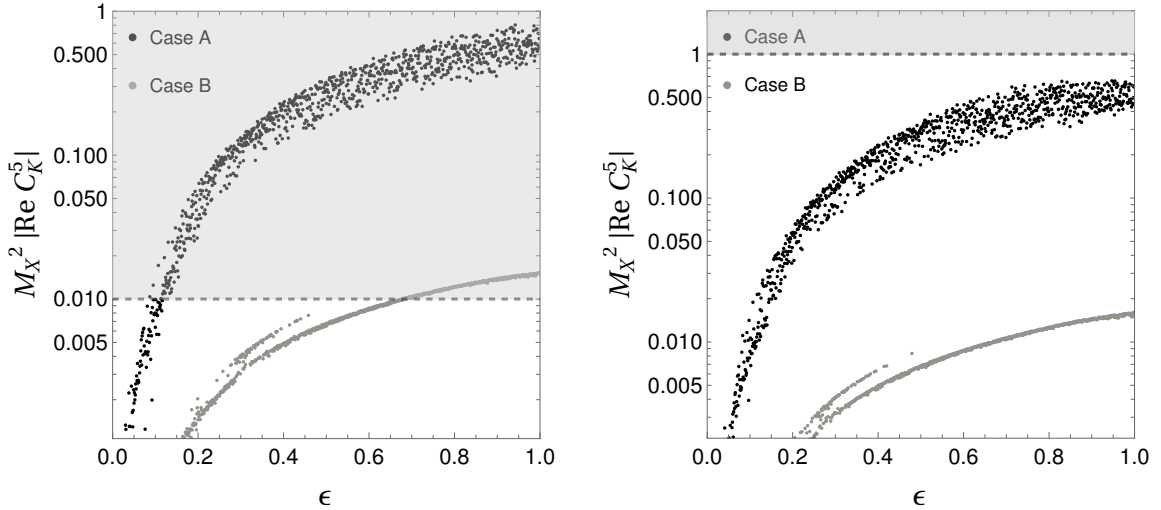


Figure 6. Magnitude of $\text{Re} C_K^5$ computed for the best-fit points for different values of ϵ and for $M_X = 10^6$ GeV (left panel) and $M_X = 10^7$ GeV (right panel). The shaded regions are excluded by the present limits at 95% confidence level.

for smaller values of ϵ in all the cases. Moreover, case B corresponding to strongly ordered μ_{di} and μ'_{di} reduces considerably the size of C_K^4 and C_K^5 . We find that the present limits on C_K^4 permit only $\epsilon < 0.15$ for case A and $M_X = 10^6$ GeV which is already disfavoured by the large χ_{\min}^2 , see Fig. 4. It is seen that case B for the same M_X can lead to solutions with acceptable χ_{\min}^2 and allowed $\text{Re} C_K^{4,5}$. For $M_X = 10^7$ GeV, both cases A and B can lead to viable solutions as can be read from Figs. 4, 5 and 6.

We find that the minimum mass the X -boson requires to evade the constraints from

Flavour observables	Experimental limit	Solution 1	Solution 2
$\text{Re}C_K^1$	$[-9.6, 9.6] \times 10^{-13}$	-5.0×10^{-16}	-8.4×10^{-16}
$\text{Im}C_K^1$	$[-9.6, 9.6] \times 10^{-13}$	-1.7×10^{-30}	1.5×10^{-29}
$\text{Re}\tilde{C}_K^1$	$[-9.6, 9.6] \times 10^{-13}$	-7.2×10^{-16}	-4.7×10^{-16}
$\text{Im}\tilde{C}_K^1$	$[-9.6, 9.6] \times 10^{-13}$	2.5×10^{-30}	3.3×10^{-30}
$\text{Re}C_K^4$	$[-3.6, 3.6] \times 10^{-15}$	-3.2×10^{-15}	-3.4×10^{-15}
$\text{Im}C_K^4$	$[-1.8, 0.9] \times 10^{-17}$	8.3×10^{-32}	4.1×10^{-29}
$\text{Re}C_K^5$	$[-1.0, 1.0] \times 10^{-14}$	-2.7×10^{-15}	-2.8×10^{-15}
$\text{Im}C_K^5$	$[-1.0, 1.0] \times 10^{-14}$	6.8×10^{-32}	3.4×10^{-29}
$ C_{B_d}^1 $	$< 2.3 \times 10^{-11}$	6.6×10^{-18}	3.3×10^{-18}
$ \tilde{C}_{B_d}^1 $	$< 2.3 \times 10^{-11}$	2.0×10^{-17}	2.9×10^{-17}
$ C_{B_d}^4 $	$< 2.1 \times 10^{-13}$	3.0×10^{-17}	2.5×10^{-17}
$ C_{B_d}^5 $	$< 6.0 \times 10^{-13}$	5.0×10^{-17}	4.2×10^{-17}
$ C_{B_s}^1 $	$< 1.1 \times 10^{-9}$	1.3×10^{-15}	3.9×10^{-15}
$ \tilde{C}_{B_s}^1 $	$< 1.1 \times 10^{-9}$	2.8×10^{-15}	5.2×10^{-14}
$ C_{B_s}^4 $	$< 1.6 \times 10^{-11}$	5.0×10^{-15}	3.7×10^{-14}
$ C_{B_s}^5 $	$< 4.5 \times 10^{-11}$	8.1×10^{-15}	6.2×10^{-14}
$ C_D^1 $	$< 7.2 \times 10^{-13}$	6.9×10^{-16}	1.3×10^{-15}
$ \tilde{C}_D^1 $	$< 7.2 \times 10^{-13}$	6.9×10^{-16}	3.9×10^{-14}
$ C_D^4 $	$< 4.8 \times 10^{-14}$	2.8×10^{-15}	2.8×10^{-14}
$ C_D^5 $	$< 4.8 \times 10^{-13}$	3.0×10^{-15}	3.1×10^{-14}
$\text{BR}[\mu \rightarrow e]$	$< 7.0 \times 10^{-13}$	5.1×10^{-17}	3.2×10^{-15}
$\text{BR}[\mu \rightarrow 3e]$	$< 1.0 \times 10^{-12}$	2.9×10^{-19}	2.0×10^{-17}
$\text{BR}[\tau \rightarrow 3\mu]$	$< 2.1 \times 10^{-8}$	5.3×10^{-19}	2.8×10^{-17}
$\text{BR}[\tau \rightarrow 3e]$	$< 2.7 \times 10^{-8}$	6.4×10^{-22}	7.2×10^{-20}
$\text{BR}[\mu \rightarrow e\gamma]$	$< 4.2 \times 10^{-13}$	6.1×10^{-21}	2.9×10^{-19}
$\text{BR}[\tau \rightarrow \mu\gamma]$	$< 4.4 \times 10^{-8}$	6.1×10^{-22}	2.4×10^{-19}
$\text{BR}[\tau \rightarrow e\gamma]$	$< 3.3 \times 10^{-8}$	7.3×10^{-24}	1.9×10^{-22}

Table 3. The magnitudes of the various Wilson coefficients (in GeV^{-2} unit) for the $\Delta F = 2$ processes in the quark sector and branching ratios for the lepton flavour violating process calculated for solutions 1 and 2. The corresponding experimental limits are also listed.

meson-antimeson oscillations, without relying on strongly ordered μ_{di} and μ'_{di} , is $M_X = 3 \times 10^6$ GeV for viable spectrum of charged fermion masses and quark mixing parameters. The strong ordering can further reduce it to $M_X = 10^6$ GeV. Example solutions for each are already given in Table 2 and 4. For these solutions, we compute all the non-vanishing C_M^i and \tilde{C}_M^i and list them in Table 3. All of them satisfy the present experimental limits. It can also be seen that the strength of Wilson coefficients corresponding to the flavour violation in the 1-2 sector is typically smaller than those in the 2-3 sector, as aimed by small ϵ in the present framework.

6.2 μ to e conversion

The X -boson, through its flavour-conserving couplings with u and d quarks and flavour violating couplings with e and μ leptons, can induce μ to e conversion within nuclei at tree-level. The branching ratio for such a transition in the nucleus field is computed in [50]. It is given by

$$\text{BR}[\mu \rightarrow e] = \frac{2G_F^2}{\omega_{\text{capt}}} (V^{(p)})^2 \left(|g_{LV}^{(p)}|^2 + |g_{RV}^{(p)}|^2 \right), \quad (6.8)$$

where the dimensionless couplings are given by

$$g_{LV,RV}^{(p)} = 2g_{LV,RV}^{(u)} + g_{LV,RV}^{(d)}, \quad (6.9)$$

with $g_{LV,RV}^{(u,d)}$ are to be identified as

$$\begin{aligned} g_{LV}^{(u,d)} &\simeq \frac{\sqrt{2}}{G_F} \frac{g_X^2}{M_X^2} (X_L^e)_{12} \frac{1}{2} \left[(X_L^{u,d})_{11} + (X_R^{u,d})_{11} \right], \\ g_{RV}^{(u,d)} &\simeq \frac{\sqrt{2}}{G_F} \frac{g_X^2}{M_X^2} (X_R^e)_{12} \frac{1}{2} \left[(X_L^{u,d})_{11} + (X_R^{u,d})_{11} \right], \end{aligned} \quad (6.10)$$

in the underlying model [51]. The functions $V^{(p)}$ and ω_{capt} in eq. (6.8) are integral involving proton distribution in the nucleus and muon capture rate by a given nucleus, respectively.

The SINDRUM II experiment [52] has obtained the most stringent limit on μ - e conversion, which uses ^{197}Au nucleus. For the latter, $V^{(p)} = 0.0974 m_\mu^{5/2}$ and $\omega_{\text{capt}} = 13.07 \times 10^6 \text{ s}^{-1}$ are estimated [50]. Using these values and substituting eqs. (6.9,6.10) in eq. (6.8), we estimate $\text{BR}[\mu \rightarrow e]$ for each point displayed in Fig. 4 corresponding to $M_X = 10^6 \text{ GeV}$. The results are displayed in the left panel of Fig. 7. We also estimate the same for the two benchmark solutions and list them in Table 3.

It can be seen that both cases A and B predict similar magnitude for $\text{BR}[\mu \rightarrow e]$. This is expected as the manipulation that differentiates between these two does not affect the flavour violating couplings in the lepton sector. $\epsilon > 0.15$ which leads to viable solutions in both cases implies $\text{BR}[\mu \rightarrow e] \leq 7 \times 10^{-15}$ which is two orders of magnitude smaller from the present limit from SINDRUM II. Therefore, the present framework does not seem to be constrained from μ to e conversion.

6.3 $l_i \rightarrow 3l_j$ and $l_i \rightarrow l_j \gamma$

The other flavour violating processes in the lepton sector include $l_i \rightarrow 3l_j$ and $l_i \rightarrow l_j \gamma$. The first is mediated by the X boson at tree-level in the present scenario, while the latter arises at one loop. The tri-lepton decays can be estimated as [51, 53]

$$\begin{aligned} \Gamma[l_i \rightarrow 3l_j] &\simeq \frac{g_X^4 m_{l_i}^5}{768\pi^3 M_X^4} \left[4\text{Re} \left((X_{eV})_{ji} (X_{eA})_{ji} (X_{eV})_{jj}^* (X_{eA})_{jj}^* \right) \right. \\ &\quad \left. + 3 \left(|(X_{eV})_{ji}|^2 + |(X_{eA})_{ji}|^2 \right) \left(|(X_{eV})_{jj}|^2 + |(X_{eA})_{jj}|^2 \right) \right], \end{aligned} \quad (6.11)$$

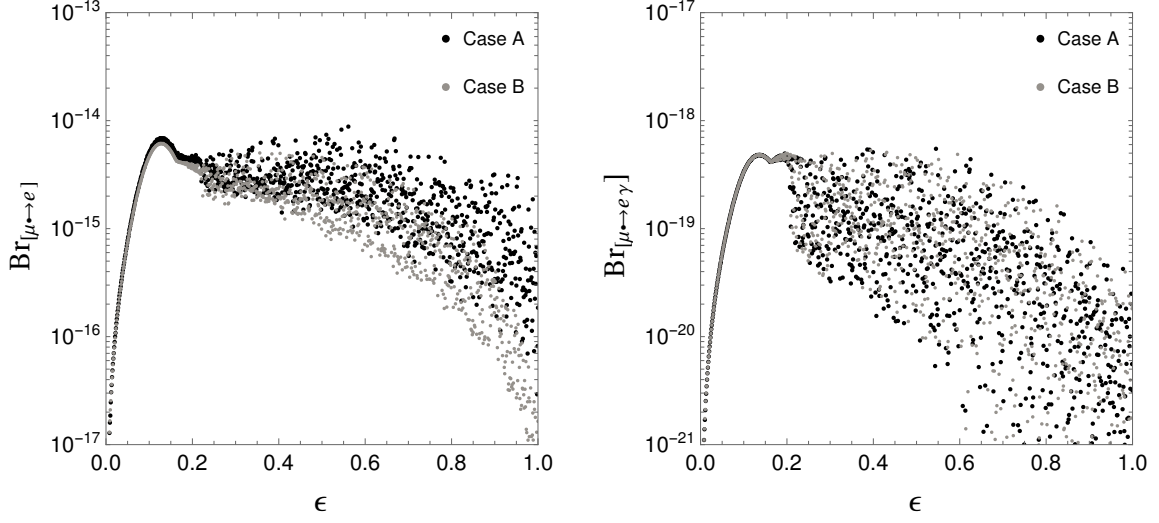


Figure 7. Left panel: $\text{BR}[\mu \rightarrow e]$ in ^{197}Au nucleus for various values of ϵ and for $M_X = 10^6$ GeV estimated from the best-fit solutions. Right panel: The same for the lepton flavour violating observable $\text{BR}[\mu \rightarrow e \gamma]$.

where, X_{eV} and X_{eA} are the vector and axial-vector couplings of the new gauge boson, respectively. In terms of the current in eq. (6.1), they are defined as:

$$X_{eV,eA} = \frac{1}{2} (X_L^e \pm X_R^e) . \quad (6.12)$$

Similarly, to compute the branching ratios for the radiative decays, $l_i \rightarrow l_j \gamma$, we use [54]:

$$\Gamma[l_i \rightarrow l_j \gamma] = \frac{\alpha g_X^4}{4\pi} \left(1 - \frac{m_{l_j}^2}{m_{l_i}^2}\right)^3 \frac{m_{l_i}^4}{M_X^4} m_{l_i} (|c_L^\gamma|^2 + |c_R^\gamma|^2) . \quad (6.13)$$

Here, α is the fine-structure constant. The coefficients c_L^γ and c_R^γ are matched to the flavour violating couplings as

$$c_L^\gamma = \sum_k Q_k \left[(X_R^e)_{jk}^* (X_R^e)_{ik} y_{RR} + (X_L^e)_{jk}^* (X_L^e)_{ik} y_{LL} \right. \\ \left. + (X_R^e)_{jk}^* (X_L^e)_{ik} y_{RL} + (X_L^e)_{jk}^* (X_R^e)_{ik} y_{LR} \right] . \quad (6.14)$$

Similarly, c_R^γ can be obtained by swapping L and R in the coupling matrices. Q_k denotes the electric charge of lepton l_k . The loop functions y_{LL} , y_{RR} , y_{LR} , and y_{RL} are given in [54].

Using eqs. (6.11) and (6.13), we can estimate the branching ratios of $\mu \rightarrow 3e$, $\tau \rightarrow 3\mu$, $\tau \rightarrow 3e$, $\mu \rightarrow e\gamma$, $\tau \rightarrow \mu\gamma$ and $\tau \rightarrow e\gamma$ in the present model. We find that, for $M_X \geq 10^6$ GeV, none of them is sizable enough to provide any meaningful constraint on the underlying model. Their estimated values for the benchmark solutions are provided in Table 3. It can be noticed again that due to the optimum arrangement of the flavour violating couplings, the flavour violation in the 1-2 sector is typically smaller or of the same size as that in the

2-3 sector. This can be considered as an improvement over the previous setups [40, 41] in which the trend is the opposite. We also give evaluated values of $\text{BR}[\mu \rightarrow e\gamma]$ for $M_X = 10^6$ GeV and several values of ϵ in Fig. 7.

In summary, the most stringent phenomenological constraint on the model comes from the $K^0\text{-}\bar{K}^0$ oscillation, which requires the new gauge boson mass at least 10^3 TeV or higher. As discussed in the previous section, the vectorlike quarks and leptons also tend to remain closer to this scale. In this scenario, all the other phenomenological constraints such as those from the direct searches and electroweak precision tests can be trivially satisfied. The reader may refer to [40] for a detailed discussion on this.

7 Neutrino masses

Although the primary focus of the study has been the charged fermion mass spectrum, we elucidate how the underlying framework can be extended to accommodate the neutrino masses. The main observational features [55–57] that make the latter different are: (a) the overall mass scale of neutrinos is several orders of magnitude smaller than that of the charged fermions, and (b) neutrinos are relatively less hierarchical since $m_{\nu 2}/m_{\nu 3} \simeq 0.2$ for $m_{\nu 1} = 0$ and $m_{\nu 2}/m_{\nu 3} \simeq 1$ for the quasi-degenerate neutrinos. As we outline below, the present framework can be extended in two qualitatively different ways to account for the neutrino masses with the aforementioned features. They are along the same lines of the usual SM extensions for the neutrino masses.

7.1 Majorana option

Neutrinos can be of Majorana nature, leading to a presence of the lepton number violation in the framework. Assuming that the scale characterizing this, namely Λ_{LN} , is greater than the electroweak as well as $U(1)_F$ breaking scale, the neutrino masses can be best described by the usual dimension-5 operator [58]. In the present framework, such operators are obtained as

$$\mathcal{L}_{\text{dim-5}} \supset \frac{c_{ij}^{(1)}}{2\Lambda_{\text{LN}}} (\bar{L}_{Li} H_{ui}) (H_{uj}^T L_{Lj}^c) + \frac{c_{ij}^{(2)}}{2\Lambda_{\text{LN}}} (\bar{L}_{Li} H_{uj}) (H_{ui}^T L_{Lj}^c) + \text{h.c.} \quad (7.1)$$

The first operator can be obtained from a full theory by integrating out fermions neutral under the SM and $U(1)_F$ gauge symmetries. This is identical to the type I seesaw mechanism [59–62]. The ultraviolet completion for the second operator requires either $U(1)_F$ neutral fermions charged under the electroweak symmetry (type III seesaw [63]) or complex scalars charged under both the electroweak and new gauge symmetry (type II seesaw [64–66]). It is straightforward to verify that none of these extensions leads to additional contributions to the anomalies.

Consequent upon the electroweak symmetry breaking, the neutrino masses are given by

$$(m_\nu)_{ij} = \frac{c_{ij}}{\Lambda_{\text{LN}}} \mu_{ui} \mu_{uj}, \quad (7.2)$$

where c_{ij} represent coefficients appearing in eq. (7.1) scaled appropriately by the Yukawa couplings y_{ui} . With the most general c_{ij} , all the three neutrinos obtain tree-level masses,

suppressed by Λ_{LN} . This is following both the features (a) and (b) mentioned at the beginning of this section. Moreover, the coefficients also provide enough freedom to reproduce the viable leptonic mixing parameters. A more predictive and insightful approach to the latter would require additional symmetries and/or structure for the specific UV completion, and it is a subject of elaborate model building.

7.2 Dirac option

Alternatively, the neutrino masses can also be introduced in an identical way it is done for the charged fermions in the framework. This minimally requires three Weyl fermions, ν_{Ri} , with $U(1)_F$ charges $(1 - \epsilon, 1 + \epsilon, -2)$ and a neutral vectorlike pair $N_{L,R}$. The former is already present in the original model from an anomaly cancellation requirement, see Table 1. All of these are singlet under the SM gauge symmetries. At the leading order, the Dirac neutrino mass matrix is obtained as

$$\left(M_\nu^{(0)}\right)_{ij} = -\frac{1}{m_N} \mu_{\nu i} \mu'_{\nu j}, \quad (7.3)$$

where $\mu_{\nu i} = y_{\nu i} \langle H_{ui} \rangle$, $\mu'_{\nu i} = y'_{\nu i} \langle \eta_i^* \rangle$ and m_N is the Dirac mass for the pair $N_{L,R}$. The above leads to one massive light neutrino state.

Because of the universal seesaw-like structure present in this framework, the smallness of the neutrino mass can be attributed to large m_N . Identifying the massive neutrino state with the atmospheric neutrino oscillation scale [57], one finds

$$m_N \approx 2 \times 10^{17} \text{ GeV} \left(\frac{0.05 \text{ eV}}{m_{\nu 3}} \right) \left(\frac{\langle \eta \rangle}{100 \text{ TeV}} \right) \left(\frac{\langle H_u \rangle}{100 \text{ GeV}} \right), \quad (7.4)$$

where we have considered all the dimensionless parameters of order one. Apparently, the issue of unnaturally small neutrino Yukawa couplings in the ordinary extension of the SM with Dirac neutrinos transforms into the issue of large hierarchy, $m_N \gg m_{U,D,E}$, in the present framework.

The solar neutrino mass scale can arise in the setup when the higher order corrections are introduced to the $M_\nu^{(0)}$. The same expression, eq. (5.4), would apply in this case with appropriate changes. However, some tuning may be required as the desired magnitude of $m_{\nu 2}/m_{\nu 3}$ is larger than the typical loop suppression factor. It is also possible to avoid this by introducing two or more copies of $N_{L,R}$ and multiplets of ν_{Ri} such that the tree-level neutrino mass matrix has rank more than one. In this case, both the solar and atmospheric scales are generated at the tree level and are expected to be not-so-hierarchical.

8 Summary and further issues

What distinguishes the framework of radiative fermion masses from other models of flavour hierarchies is its ability to provide at least some of the fermion masses as calculable quantities. Here, calculability means that these masses can be fully or partially expressed in terms of quantities that can be measured independently in experiments, at least in principle. Such quantities must arise from new physics interactions, as the standard model alone cannot

accommodate the radiative mass mechanism. This opens up an avenue for model building aimed at constructing viable and predictive models for radiative mass generation. In the present work, we systematically explore the new gauge sector that can enable this.

It is shown that the SM extended with just a single abelian gauge symmetry is sufficient to provide a suitable framework for the radiative induction of the masses of the lighter generations. The Yukawa sector at the tree level can be engineered to possess a global $U(2)^5$ symmetry corresponding to the massless first and second generations. This symmetry does not commute with the flavour-dependent gauge symmetry, and it gets broken completely if all three generations of the SM fermions are charged differently under the latter. This then generates the masses of the second generation at one loop and of the first generation at two loops. The 2-loop corrected mass matrix can be completely expressed in terms of tree-level mass matrix and the gauge charges and gauge boson mass, as shown in eq. (2.39). This offers significant advancements over our previous attempts in this direction, in which the masses of both the lighter generations were induced at one-loop and inter-generational hierarchy was attributed to specific ordering in the gauge boson masses. These models also required enlarged gauge sector in comparison to the one presented here.

Large flavour changing neutral currents mediated by the gauge boson of new gauge symmetry are inherently present in this kind of framework. They put the strongest constraint on the scale of new physics. As we have shown in this study, the flavour changing couplings can be ordered in such a way that their strengths in the 1-2 sector are the smallest. This is phenomenologically favourable since the most stringent constraint on flavour violations comes from the 1-2 sector, in particular, from $K^0-\bar{K}^0$ mixing and $\mu-e$ conversion in nuclei. The smallness of flavour changing couplings in 1-2 is proportional to the difference between the charges of the first and second-generation fermions under the new gauge symmetry. The latter cannot be made arbitrarily small, as complete degeneracy in these charges leads to the strictly massless first generation. This correlation is then explored to find the optimum strength of flavour violation through a comprehensive numerical analysis, and we find that the down-type quark sector predominantly governs this optimization. If the down quark mass is to be reproduced within the 3σ range of its present value extracted from the lattice computation, then the mass of the $U(1)_F$ gauge boson can not be lower than 10^3 TeV provided that all the flavour constraints are satisfied. This lower limit is smaller by nearly two orders of magnitude in comparison to our previous frameworks proposed along the same lines [40, 41].

It is remarkable that extending the SM with a single abelian gauge symmetry can enable its gauge sector to support radiative mass generation for lighter fermions. However, there are areas where this framework requires further improvement. For example,

- Calculability is not fully achieved because the Yukawa sector of the theory still contains numerous couplings. These couplings may be reduced if $U(1)_F$ is replaced with a gauge symmetry under which the three generations transform as an irreducible representation (see, for example, [41]). However, this would enrich the gauge sector, and it remains to be seen whether the salient features of the minimal gauge sector presented here can be retained. Another option to reduce Yukawa couplings to some

extent is to implement this scheme in models that provide quark-lepton unification [67–69] at high energies.

- Although the framework accounts for the hierarchical nature of charged fermion masses, it does not explain the smallness of mixing in the quark sector. This is because the underlying symmetries and the field content of the model allow different and arbitrary tree-level Yukawa couplings for the up-type and down-type quarks. Frameworks with an improved degree of calculability can address this issue.
- The lowest scale of new physics remains at 10^3 TeV. While this scale, or even a larger one, does not hinder the core mechanism discussed here, the significant separation between it and the electroweak scale poses a challenge. This separation can be managed at the expense of fine-tuning in the generic case. However, in more ambitious theories where the parameters of the scalar potential are also calculable, this becomes a concrete problem.

We believe that the above issues require a set of systematic investigations to establish further the validity and robustness of the radiative mass generation scheme.

Acknowledgements

This work is supported by the Department of Space (DOS), Government of India. KMP acknowledges partial support under the MATRICS project (MTR/2021/000049) from the Science & Engineering Research Board (SERB), Department of Science and Technology (DST), Government of India.

A On the origin of the gauge charges

A choice made in eq. (4.1) for the charges of underlying abelian flavour symmetry can simply be obtained from kinetic mixing. Consider two $U(1)$ symmetries with gauge bosons $X_{1,2}^\mu$ and the gauge interactions

$$-\mathcal{L}_G = g^{(1)} q_{ii}^{(1)} \bar{f}'_i \gamma^\mu f'_i X_\mu^{(1)} + g^{(2)} q_{ii}^{(2)} \bar{f}'_i \gamma^\mu f'_i X_\mu^{(2)}, \quad (\text{A.1})$$

where f' stands for both f'_L and f'_R . An appropriate choice for the charge matrices is

$$q^{(1)} = \text{Diag.}(1, 1, -2), \quad q^{(2)} = \text{Diag.}(1, -1, 0). \quad (\text{A.2})$$

Next, consider the kinetic terms of these gauge bosons with non-vanishing kinetic mixing [70]

$$-\mathcal{L}_{\text{kin}} = \frac{1}{4} F_{\mu\nu}^{(1)} F^{(1)\mu\nu} + \frac{1}{4} F_{\mu\nu}^{(2)} F^{(2)\mu\nu} + \frac{\chi}{2} F_{\mu\nu}^{(1)} F^{(2)\mu\nu}, \quad (\text{A.3})$$

with $F_{\mu\nu}^{(\alpha)}$ denote the field strength of the gauge boson $X_\mu^{(\alpha)}$. The kinetic terms can be diagonalized by a linear transformation

$$\begin{pmatrix} X_\mu^{(1)} \\ X_\mu^{(2)} \end{pmatrix} \rightarrow \begin{pmatrix} 1 & 0 \\ -\chi & 1 \end{pmatrix} \begin{pmatrix} X_\mu^{(1)} \\ X_\mu^{(2)} \end{pmatrix}. \quad (\text{A.4})$$

This removes the kinetic mixing from the kinetic terms, which then reappear in the gauge interactions. Substituting (A.4) in eq. (A.1) leads to

$$-\mathcal{L}_G = g^{(1)} \left(q_{ii}^{(1)} - \chi \frac{g^{(2)}}{g^{(1)}} q_{ii}^{(2)} \right) \bar{f}'_i \gamma^\mu f'_i X_\mu^{(1)} + g^{(2)} q_{ii}^{(2)} \bar{f}'_i \gamma^\mu f'_i X_\mu^{(2)}. \quad (\text{A.5})$$

Setting $g^{(1)} = g_X$, $\chi g^{(2)}/g^{(1)} \equiv \epsilon$ and $X_\mu^{(1)} = X_\mu$, one obtains the desired charges given in eq. (4.1). By setting $M_{X_2} \gg M_X$, the effects of the gauge interactions associated with $X_\mu^{(2)}$ gauge boson can be decoupled from the effective theory.

The two $U(1)$ symmetries with flavour non-universal charges in eq. (A.2) along with any flavour universal $U(1)$ (for example hypercharge in the present framework) can be recast into $U(1)_1 \times U(1)_2 \times U(1)_3$ such that only i^{th} generation is charged under $U(1)_i$. To see this, consider gauge interactions:

$$\sum_{\alpha=1}^3 g^{(\alpha)} q_{ii}^{(\alpha)} \bar{f}'_i \gamma^\mu f'_i X_\mu^{(\alpha)}, \quad (\text{A.6})$$

with $q^{(1),(2)}$ as already given in eq. (A.2) and $q^{(3)} = \text{Diag.}(1, 1, 1)$. A rotation

$$X_\mu^{(\alpha)} \rightarrow \tilde{X}_\mu^{(\alpha)} = \mathcal{R}_{\alpha\beta} X_\mu^{(\beta)}, \quad (\text{A.7})$$

can be performed to redefine the gauge bosons such that in the new basis, the gauge interactions become

$$\sum_{\alpha=1}^3 \tilde{g}^{(\alpha)} \tilde{q}_{ii}^{(\alpha)} \bar{f}'_i \gamma^\mu f'_i \tilde{X}_\mu^{(\alpha)}. \quad (\text{A.8})$$

The new couplings are then given by

$$\tilde{g}^{(\alpha)} \tilde{q}_{ii}^{(\alpha)} = \mathcal{R}_{\alpha\beta} g^{(\beta)} q_{ii}^{(\beta)}, \quad (\text{A.9})$$

where \mathcal{R} is an orthogonal matrix.

For a specific choice, $\sqrt{6}g^{(1)} = \sqrt{2}g^{(2)} = \sqrt{3}g^{(3)} \equiv \tilde{g}$, and

$$\mathcal{R} = \begin{pmatrix} \frac{1}{\sqrt{6}} & \frac{1}{\sqrt{2}} & \frac{1}{\sqrt{3}} \\ \frac{1}{\sqrt{6}} & -\frac{1}{\sqrt{2}} & \frac{1}{\sqrt{3}} \\ -\sqrt{\frac{2}{3}} & 0 & \frac{1}{\sqrt{3}} \end{pmatrix}, \quad (\text{A.10})$$

one finds,

$$\tilde{g}^{(1)} \tilde{q}^{(1)} = \tilde{g} \text{Diag.}(1, 0, 0), \quad \tilde{g}^{(2)} \tilde{q}^{(2)} = \tilde{g} \text{Diag.}(0, 1, 0), \quad \tilde{g}^{(3)} \tilde{q}^{(3)} = \tilde{g} \text{Diag.}(0, 0, 1). \quad (\text{A.11})$$

Therefore, the three abelian symmetries of the underlying theory, i.e. two flavour non-universal new abelian symmetries and a hypercharge, can be put in a form such that each generation is exclusively charged under only one $U(1)$ with equal strength of interactions. Recently, this kind of framework has been put forward under the name of “tri-hypercharge” [45] or “deconstructed hypercharge” [46].

B Scalar sector

In this Appendix, we discuss the scalar sector of the framework and outline its phenomenological implications. The model contains total nine scalar multiplets, H_{ui} , H_{di} and η_i with $i = 1, 2, 3$. The SM and $U(1)_F$ invariant renormalisable scalar potential can be written as:

$$\begin{aligned}
V = & m_{ui}^2 H_{ui}^\dagger H_{ui} + m_{di}^2 H_{di}^\dagger H_{di} + m_{\eta i}^2 \eta_i^\dagger \eta_i \\
& + \{ (m_{ud\eta})_{ijk} \epsilon_{ijk} \eta_i H_{uj} H_{dk} + (m_\eta)_{ijk} \epsilon_{ijk} \eta_i \eta_j \eta_k + \text{h.c.} \} \\
& + (\lambda_u)_{ij} H_{ui}^\dagger H_{ui} H_{uj}^\dagger H_{uj} + (\lambda_d)_{ij} H_{di}^\dagger H_{di} H_{dj}^\dagger H_{dj} + (\lambda_\eta)_{ij} \eta_i^\dagger \eta_i \eta_j^\dagger \eta_j \\
& + (\lambda_{ud})_{ij} H_{ui}^\dagger H_{ui} H_{dj}^\dagger H_{dj} + (\lambda_{u\eta})_{ij} H_{ui}^\dagger H_{ui} \eta_j^\dagger \eta_j + (\lambda_{d\eta})_{ij} H_{di}^\dagger H_{di} \eta_j^\dagger \eta_j \\
& + (\tilde{\lambda}_{ud})_{ij} H_{ui}^\dagger H_{uj} H_{dj}^\dagger H_{di} + (\tilde{\lambda}_{u\eta})_{ij} H_{ui}^\dagger H_{uj} \eta_j^\dagger \eta_i + (\tilde{\lambda}_{d\eta})_{ij} H_{di}^\dagger H_{dj} \eta_j^\dagger \eta_i \\
& + \left\{ (\lambda_{ud\eta})_{ij} \eta_i^\dagger H_{ui} \eta_j^\dagger H_{dj} + (\tilde{\lambda}_{ud\eta})_{ij} \eta_i^\dagger H_{uj} \eta_j^\dagger H_{di} + \text{h.c.} \right\}. \tag{B.1}
\end{aligned}$$

Note that the above potential is identical to the one obtained in our previous framework based on two flavour non-universal abelian symmetries [40]. Consequent upon the gauge symmetry breaking this leads to several electrically charged and neutral physical scalars. In principle, these states can also contribute to the charged fermion masses through loops. However, such contributions can remain relatively suppressed under reasonable conditions as we discuss below.

Identifying the electromagnetically neutral scalars residing in H_{ui} , H_{di} and η_i as h_{ui} , h_{di} and η_i , respectively, their mass term can be parametrized as

$$\frac{1}{2} (M_h^2)_{ab} \tilde{h}_a \tilde{h}_b, \tag{B.2}$$

where $a = 1, \dots, 9$ and $\tilde{h} = (h_{ui}, h_{dj}, \eta_k)^T$. The 9×9 symmetric neutral scalar mass matrix M_h^2 can be written in terms of 3×3 blocks as

$$M_h^2 = \begin{pmatrix} m_{uu}^2 & m_{ud}^2 & m_{u\eta}^2 \\ (m_{ud}^2)^T & m_{dd}^2 & m_{d\eta}^2 \\ (m_{u\eta}^2)^T & (m_{d\eta}^2)^T & m_{\eta\eta}^2 \end{pmatrix}. \tag{B.3}$$

The above parameters can be computed from the scalar potential and they are functions of various parameters appearing in eq. (B.1) and VEVs of H_{ui} , H_{di} and η_i . As usual, the physical neutral scalar states h_a can be obtained by diagonalizing M_h^2 . Explicitly, we define

$$\tilde{h}_a = (R_h)_{ab} h_b, \tag{B.4}$$

where R_h is orthogonal matrix such that $R_h^T M_h^2 R_h = \text{Diag.}(m_{h_1}^2, \dots, m_{h_9}^2)$. Although the typical mass scale of the scalars is $\mathcal{O}(M_X)$, one of them must be identified with the observed SM-like Higgs boson with a mass of 125 GeV [71]. Minimally, the lightest of the neutral scalars, h_1 , can play this role. This requires $\text{Det.} M_h^2 \ll M_X^{18}$, necessitating a tuning of the parameters in the scalar potential. Given the large number of incalculable parameters in the scalar potential, we assume that such an arrangement is possible. As noted in section 8,

this becomes a concrete problem in more ambitious frameworks where the scalar potential is better constrained.

Let us first comment on the loop-induced contributions of these scalars to the fermion masses. Since the left-chiral fermions of the SM couple only to H_{ui} or H_{di} , and the right-chiral fermions couple solely to η_i at tree-level (see eq. (5.1)), the one-loop diagrams mediated by the neutral scalars depend on the mixing between $H_{ui,di}$ and η_i . These contributions can be small if $m_{\eta\eta}^2 \gg m_{u\eta}^2, m_{d\eta}^2$ in eq. (B.2). In this limit, the physical states $h_{1,\dots,6}$ ($h_{7,\dots,9}$) consist of dominantly $H_{ui,di}$ (η_i) with components of η_i ($H_{ui,di}$) suppressed by a factor of $\mathcal{O}(m_{d\eta}^2(m_{\eta\eta}^2)^{-1})$ or $\mathcal{O}(m_{u\eta}^2(m_{\eta\eta}^2)^{-1})$. Hence, h_a mediated diagrams can provide only sub-leading contributions to $\delta M^{(1,2)}$. The same argument also applies to the charged scalars. As they arise entirely from H_{di} and H_{ui} with no counterparts in η_i to mix with, they do not contribute to the fermion masses at 1-loop. Thus, the scalar-induced contributions in this setup can be made suppressed if small enough mixing between $H_{ui,di}$ and η_i is considered.

The multiplicity of scalars and the feature that Yukawa couplings are not proportional to the masses for the SM fermions in the underlying framework leads to flavour-changing transitions mediated by the neutral scalars. For example, consider the interactions involving the up-type quarks in eq. (5.1). In the physical basis, they lead to the following flavour changing interactions between the SM up-type quarks and neutral scalars:

$$\left(\left(U_L^{u\dagger} \right)_{mi} y_{ui} (R_u)_{ia} \left(\rho_R^\dagger U_R^u \right)_n + \left(U_L^{u\dagger} \rho_L \right)_m y'_{uk} (R_\eta)_{ka} (U_R^u)_{kn} \right) \bar{u}_{Lm} h_a u_{Rn} + \text{h.c.}, \quad (\text{B.5})$$

at the leading order. Since the masses of the heavy neutral scalars are $\gtrsim \mathcal{O}(10^6)$ GeV, the FCNCs mediated by them are sufficiently small. The existing experimental constraints therefore only require that the flavor-changing couplings of the light Higgs be suppressed. Given the large number of parameters in the scalar potential, we assume that such an arrangement is possible, albeit with some fine-tuning.

C Details of numerical analysis

It can be seen from the Lagrangian in eq. (5.1) that the parameters m_U , m_D and m_E can be made real by absorbing their phases into the fields U_L , D_L and E_L , respectively. Similarly, rephasing of Q_{Li} , L_{Li} , u_{Ri} , d_{Ri} and e_{Ri} can get rid of unphysical phases of y_{ui} , y_{ei} , y'_{ui} , y'_{di} and y'_{ei} , respectively. The parameter y_{d3} can also be made real by rephasing D_R . Furthermore, we assume that all the VEVs are real. The gauge sector has three real parameters, g_X , ϵ and M_X , out of which g_X can be fixed to some particular value without loss of generality and the remaining two parameters then control the strength of loop corrections. Hence, the model has 25 real parameters, i.e. real ϵ , M_X , m_U , m_D , m_E , μ_{ui} , μ_{ei} , μ'_{ui} , μ'_{di} , μ'_{ei} , μ_{d3} and complex μ_{d1} , μ_{d2} . These can be used to reproduce 13 observed quantities which include 9 charged fermion masses, 3 quark mixing angles and a Dirac CP phase in the quark sector.

Parameters	Solution 1	Solution 2
M_X	3×10^6	10^6
ϵ	0.178	0.285
m_U	5.6653×10^6	6.2838×10^6
m_D	4.9336×10^8	1.5524×10^8
m_E	8.2489×10^6	3.9884×10^6
μ_{u1}	-9.6518	1.2821
μ_{u2}	9.9336	-7.2968
μ_{u3}	-3.7757×10^2	4.6534×10^2
μ'_{u1}	6.9209×10^5	1.1248×10^6
μ'_{u2}	-1.6434×10^6	-1.4161×10^6
μ'_{u3}	-1.8288×10^6	1.4585×10^6
μ_{d1}	$-1.8003 \times 10^1 + i \ 2.4815$	$1.9233 + i \ 1.9146$
μ_{d2}	$2.9553 \times 10^1 + i \ 1.6954$	$-3.2718 + i \ 1.9150 \times 10^1$
μ_{d3}	-2.2993×10^2	2.2572×10^2
μ'_{d1}	-7.1617×10^5	-4.8001×10^4
μ'_{d2}	7.2368×10^5	4.8498×10^5
μ'_{d3}	4.4255×10^6	1.4044×10^6
μ_{e1}	2.5748×10^1	-1.3349×10^1
μ_{e2}	-2.6008×10^1	-1.5363×10^1
μ_{e3}	-4.7027×10^1	2.1028×10^1
μ'_{e1}	-1.3925×10^5	3.6639×10^4
μ'_{e2}	-1.4093×10^5	-7.9852×10^4
μ'_{e3}	-1.4252×10^5	-2.1704×10^5

Table 4. Optimized values of various input parameters obtained for two example solutions displayed in Table 2. All the values of dimension-full parameters are in GeV.

The fitting of observables is carried out using the χ^2 optimization procedure. The χ^2 function is defined as

$$\chi^2 = \sum_i \left(\frac{O_{\text{th}}^i - O_{\text{exp}}^i}{\sigma_i} \right)^2, \quad (\text{C.1})$$

where $i = 1, \dots, 13$ represents the thirteen observables. O_{th}^i is the theoretically computed value of the i^{th} observable in terms of the input parameters listed above. We carry out this computation at the renormalization scale $Q = M_Z$ as discussed in section 5. O_{exp}^i (σ^i) are the corresponding mean (standard deviation) value extracted from the experiments and evolved at $Q = M_Z$. The values of charged fermion masses are taken from [72] and quark mixing parameters from [73]. Note that for the charged lepton masses, we use conservative 10% uncertainty, as done before in [40, 41, 74]. All these values are listed in the second column in Table 2 for convenience and comparison.

While performing the optimization, we also ensure that various parameters do not take

unrealistic values. For example, the perturbativity limits would imply $y_{fi} \leq \sqrt{4\pi}$. Since $\langle H_{fi} \rangle$ contributes to the electroweak symmetry breaking, one expects $\langle H_{fi} \rangle < 246$ GeV. Therefore, we impose that $\mu_{fi} < \sqrt{4\pi} \times 246$ GeV. Similarly, $\mu'_{fi} < \sqrt{4\pi} M_X$ is also imposed, since these parameters break the $U(1)_F$ symmetry and hence their values cannot be significantly higher than the underlying symmetry breaking scale. The masses of vectorlike fermions do not break any symmetry, and hence they are kept unrestricted.

The fitted values of various input parameters for two example solutions as discussed in section 5.2 are displayed here in Table 4. Both the solutions correspond to the lowest possible allowed values of ϵ for which $\chi^2_{\min} \lesssim 5$.

References

- [1] S. Weinberg, *Electromagnetic and weak masses*, *Phys. Rev. Lett.* **29** (1972) 388.
- [2] H. Georgi and S.L. Glashow, *Attempts to calculate the electron mass*, *Phys. Rev. D* **7** (1973) 2457.
- [3] R.N. Mohapatra, *Gauge Model for Chiral Symmetry Breaking and Muon electron Mass Ratio*, *Phys. Rev. D* **9** (1974) 3461.
- [4] S.M. Barr and A. Zee, *Calculating the Electron Mass in Terms of Measured Quantities*, *Phys. Rev. D* **17** (1978) 1854.
- [5] F. Wilczek and A. Zee, *Horizontal Interaction and Weak Mixing Angles*, *Phys. Rev. Lett.* **42** (1979) 421.
- [6] T. Yanagida, *Horizontal Symmetry and Mass of the Top Quark*, *Phys. Rev. D* **20** (1979) 2986.
- [7] R. Barbieri and D.V. Nanopoulos, *Hierarchical Fermion Masses From Grand Unification*, *Phys. Lett. B* **95** (1980) 43.
- [8] B.S. Balakrishna, *Fermion Mass Hierarchy From Radiative Corrections*, *Phys. Rev. Lett.* **60** (1988) 1602.
- [9] B.S. Balakrishna, A.L. Kagan and R.N. Mohapatra, *Quark Mixings and Mass Hierarchy From Radiative Corrections*, *Phys. Lett. B* **205** (1988) 345.
- [10] B.S. Balakrishna, *RADIATIVELY INDUCED LEPTON MASSES*, *Phys. Lett. B* **214** (1988) 267.
- [11] B.S. Balakrishna and R.N. Mohapatra, *Radiative Fermion Masses From New Physics at TeV Scale*, *Phys. Lett. B* **216** (1989) 349.
- [12] K.S. Babu and X.-G. He, *Fermion mass hierarchy and the strong CP problem*, *Phys. Lett. B* **219** (1989) 342.
- [13] K.S. Babu, B.S. Balakrishna and R.N. Mohapatra, *Supersymmetric Model for Fermion Mass Hierarchy*, *Phys. Lett. B* **237** (1990) 221.
- [14] R. Rattazzi, *Radiative quark masses constrained by the gauge group only*, *Z. Phys. C* **52** (1991) 575.
- [15] Z.G. Berezhiani and R. Rattazzi, *Universal seesaw and radiative quark mass hierarchy*, *Phys. Lett. B* **279** (1992) 124.

- [16] Z. Berezhiani and R. Rattazzi, *Inverted radiative hierarchy of quark masses*, *JETP Lett.* **56** (1992) 429.
- [17] Z.G. Berezhiani and R. Rattazzi, *Inverse hierarchy approach to fermion masses*, *Nucl. Phys. B* **407** (1993) 249 [[hep-ph/9212245](#)].
- [18] N. Arkani-Hamed, H.-C. Cheng and L.J. Hall, *A Supersymmetric theory of flavor with radiative fermion masses*, *Phys. Rev. D* **54** (1996) 2242 [[hep-ph/9601262](#)].
- [19] S.M. Barr, *Radiative fermion mass hierarchy in a non-supersymmetric unified theory*, *Phys. Rev. D* **76** (2007) 105024 [[0706.1490](#)].
- [20] P.W. Graham and S. Rajendran, *A Domino Theory of Flavor*, *Phys. Rev. D* **81** (2010) 033002 [[0906.4657](#)].
- [21] B.A. Dobrescu and P.J. Fox, *Quark and lepton masses from top loops*, *JHEP* **08** (2008) 100 [[0805.0822](#)].
- [22] A. Crivellin, J. Girrbach and U. Nierste, *Yukawa coupling and anomalous magnetic moment of the muon: an update for the LHC era*, *Phys. Rev. D* **83** (2011) 055009 [[1010.4485](#)].
- [23] A. Crivellin, L. Hofer, U. Nierste and D. Scherer, *Phenomenological consequences of radiative flavor violation in the MSSM*, *Phys. Rev. D* **84** (2011) 035030 [[1105.2818](#)].
- [24] R. Adhikari, D. Borah and E. Ma, *New $U(1)$ Gauge Model of Radiative Lepton Masses with Sterile Neutrino and Dark Matter*, *Phys. Lett. B* **755** (2016) 414 [[1512.05491](#)].
- [25] C.-W. Chiang and K. Yagyu, *Radiative Seesaw Mechanism for Charged Leptons*, *Phys. Rev. D* **103** (2021) L111302 [[2104.00890](#)].
- [26] C.-W. Chiang, R. Obuchi and K. Yagyu, *Dark sector as origin of light lepton mass and its phenomenology*, *JHEP* **05** (2022) 070 [[2202.07784](#)].
- [27] M.J. Baker, P. Cox and R.R. Volkas, *Has the Origin of the Third-Family Fermion Masses been Determined?*, *JHEP* **04** (2021) 151 [[2012.10458](#)].
- [28] M.J. Baker, P. Cox and R.R. Volkas, *Radiative muon mass models and $(g - 2)_\mu$* , *JHEP* **05** (2021) 174 [[2103.13401](#)].
- [29] W. Yin, *Radiative lepton mass and muon $g - 2$ with suppressed lepton flavor and CP violations*, *JHEP* **08** (2021) 043 [[2103.14234](#)].
- [30] W.-F. Chang, *Non-universal gauged lepton number for charged lepton masses hierarchy and $(g - 2)_{e,\mu}$* , [2210.11097](#).
- [31] Y. Zhang, *The minimal flavor structure of quarks and leptons*, *J. Phys. G* **50** (2023) 125006 [[2302.05943](#)].
- [32] A. Greljo and A.E. Thomsen, *Rising through the ranks: flavor hierarchies from a gauged $SU(2)$ symmetry*, *Eur. Phys. J. C* **84** (2024) 213 [[2309.11547](#)].
- [33] C. Arbeláez, A.E. Cárcamo Hernández, C. Dib, P. Escalona Contreras, V.K. N. and A. Zerwekh, *A common framework for fermion mass hierarchy, leptogenesis and dark matter*, [2404.06577](#).
- [34] A. Greljo, A.E. Thomsen and H. Tiblom, *Flavor Hierarchies From $SU(2)$ Flavor and Quark-Lepton Unification*, [2406.02687](#).
- [35] R. Kuchimanchi, *Parity and Lepton Masses in the Left Right Symmetric Model*, [2406.14480](#).

- [36] A. Hernandez Galeana and J.H. Montes de Oca Yemha, *Radiative generation of light fermion masses in a $SU(3)(H)$ horizontal symmetry model*, *Rev. Mex. Fis.* **50** (2004) 522 [[hep-ph/0406315](#)].
- [37] M. Reig, J.W.F. Valle and F. Wilczek, *$SO(3)$ family symmetry and axions*, *Phys. Rev. D* **98** (2018) 095008 [[1805.08048](#)].
- [38] S. Weinberg, *Models of Lepton and Quark Masses*, *Phys. Rev. D* **101** (2020) 035020 [[2001.06582](#)].
- [39] S. Jana, S. Klett and M. Lindner, *Flavor seesaw mechanism*, *Phys. Rev. D* **105** (2022) 115015 [[2112.09155](#)].
- [40] G. Mohanta and K.M. Patel, *Radiatively generated fermion mass hierarchy from flavor nonuniversal gauge symmetries*, *Phys. Rev. D* **106** (2022) 075020 [[2207.10407](#)].
- [41] G. Mohanta and K.M. Patel, *Gauged $SU(3)_F$ and loop induced quark and lepton masses*, *JHEP* **10** (2023) 128 [[2308.05642](#)].
- [42] Z.G. Berezhiani, *The Weak Mixing Angles in Gauge Models with Horizontal Symmetry: A New Approach to Quark and Lepton Masses*, *Phys. Lett. B* **129** (1983) 99.
- [43] Z.G. Berezhiani, *Horizontal Symmetry and Quark - Lepton Mass Spectrum: The $SU(5) \times SU(3)$ -h Model*, *Phys. Lett. B* **150** (1985) 177.
- [44] D. Chang and R.N. Mohapatra, *Small and Calculable Dirac Neutrino Mass*, *Phys. Rev. Lett.* **58** (1987) 1600.
- [45] M. Fernández Navarro and S.F. King, *Tri-hypercharge: a separate gauged weak hypercharge for each fermion family as the origin of flavour*, *JHEP* **08** (2023) 020 [[2305.07690](#)].
- [46] J. Davighi and B.A. Stefanek, *Deconstructed hypercharge: a natural model of flavour*, *JHEP* **11** (2023) 100 [[2305.16280](#)].
- [47] UTFIT collaboration, *Model-independent constraints on $\Delta F = 2$ operators and the scale of new physics*, *JHEP* **03** (2008) 049 [[0707.0636](#)].
- [48] M. Ciuchini et al., *Delta $M(K)$ and epsilon(K) in SUSY at the next-to-leading order*, *JHEP* **10** (1998) 008 [[hep-ph/9808328](#)].
- [49] D. Becirevic, M. Ciuchini, E. Franco, V. Gimenez, G. Martinelli, A. Masiero et al., *$B_d - \bar{B}_d$ mixing and the $B_d \rightarrow J/\psi K_s$ asymmetry in general SUSY models*, *Nucl. Phys. B* **634** (2002) 105 [[hep-ph/0112303](#)].
- [50] R. Kitano, M. Koike and Y. Okada, *Detailed calculation of lepton flavor violating muon electron conversion rate for various nuclei*, *Phys. Rev. D* **66** (2002) 096002 [[hep-ph/0203110](#)].
- [51] A. Smolkovič, M. Tamaro and J. Zupan, *Anomaly free Froggatt-Nielsen models of flavor*, *JHEP* **10** (2019) 188 [[1907.10063](#)].
- [52] SINDRUM II collaboration, *A Search for muon to electron conversion in muonic gold*, *Eur. Phys. J. C* **47** (2006) 337.
- [53] J. Heeck, *Lepton flavor violation with light vector bosons*, *Phys. Lett. B* **758** (2016) 101 [[1602.03810](#)].
- [54] L. Lavoura, *General formulae for $f(1) \rightarrow f(2)$ gamma*, *Eur. Phys. J. C* **29** (2003) 191 [[hep-ph/0302221](#)].

- [55] F. Capozzi, E. Di Valentino, E. Lisi, A. Marrone, A. Melchiorri and A. Palazzo, *Global constraints on absolute neutrino masses and their ordering*, *Phys. Rev. D* **95** (2017) 096014 [[2003.08511](#)].
- [56] P.F. de Salas, D.V. Forero, S. Gariazzo, P. Martínez-Miravé, O. Mena, C.A. Ternes et al., *2020 global reassessment of the neutrino oscillation picture*, *JHEP* **02** (2021) 071 [[2006.11237](#)].
- [57] I. Esteban, M.C. Gonzalez-Garcia, M. Maltoni, T. Schwetz and A. Zhou, *The fate of hints: updated global analysis of three-flavor neutrino oscillations*, *JHEP* **09** (2020) 178 [[2007.14792](#)].
- [58] S. Weinberg, *Baryon and Lepton Nonconserving Processes*, *Phys. Rev. Lett.* **43** (1979) 1566.
- [59] P. Minkowski, $\mu \rightarrow e\gamma$ at a Rate of One Out of 10^9 Muon Decays?, *Phys. Lett. B* **67** (1977) 421.
- [60] T. Yanagida, *Horizontal gauge symmetry and masses of neutrinos*, *Conf. Proc. C* **7902131** (1979) 95.
- [61] R.N. Mohapatra and G. Senjanovic, *Neutrino Mass and Spontaneous Parity Nonconservation*, *Phys. Rev. Lett.* **44** (1980) 912.
- [62] J. Schechter and J.W.F. Valle, *Neutrino Masses in $SU(2) \times U(1)$ Theories*, *Phys. Rev. D* **22** (1980) 2227.
- [63] R. Foot, H. Lew, X.G. He and G.C. Joshi, *Seesaw Neutrino Masses Induced by a Triplet of Leptons*, *Z. Phys. C* **44** (1989) 441.
- [64] G. Lazarides, Q. Shafi and C. Wetterich, *Proton Lifetime and Fermion Masses in an $SO(10)$ Model*, *Nucl. Phys. B* **181** (1981) 287.
- [65] M. Magg and C. Wetterich, *Neutrino Mass Problem and Gauge Hierarchy*, *Phys. Lett. B* **94** (1980) 61.
- [66] R.N. Mohapatra and G. Senjanovic, *Neutrino Masses and Mixings in Gauge Models with Spontaneous Parity Violation*, *Phys. Rev. D* **23** (1981) 165.
- [67] H. Georgi and S.L. Glashow, *Unity of All Elementary Particle Forces*, *Phys. Rev. Lett.* **32** (1974) 438.
- [68] H. Fritzsch and P. Minkowski, *Unified Interactions of Leptons and Hadrons*, *Annals Phys.* **93** (1975) 193.
- [69] J.C. Pati and A. Salam, *Lepton Number as the Fourth Color*, *Phys. Rev. D* **10** (1974) 275.
- [70] B. Holdom, *Two $U(1)$'s and Epsilon Charge Shifts*, *Phys. Lett. B* **166** (1986) 196.
- [71] ATLAS, CMS collaboration, *Combined Measurement of the Higgs Boson Mass in pp Collisions at $\sqrt{s} = 7$ and 8 TeV with the ATLAS and CMS Experiments*, *Phys. Rev. Lett.* **114** (2015) 191803 [[1503.07589](#)].
- [72] Z.-z. Xing, H. Zhang and S. Zhou, *Updated Values of Running Quark and Lepton Masses*, *Phys. Rev. D* **77** (2008) 113016 [[0712.1419](#)].
- [73] PARTICLE DATA GROUP collaboration, *Review of Particle Physics*, *PTEP* **2022** (2022) 083C01.
- [74] V.S. Mummidi and K.M. Patel, *Leptogenesis and fermion mass fit in a renormalizable $SO(10)$ model*, *JHEP* **12** (2021) 042 [[2109.04050](#)].